THE JOURNAL OF PHYSICAL CHEMISTRY C

Article

Cite This: J. Phys. Chem. C XXXX, XXX, XXX−XXX

pubs.acs.org/JPCC

Low-Vapor-Pressure Solvent Additives Function as Polymer Swelling Agents in Bulk Heterojunction Organic Photovoltaics

Matthew T. Fontana,[†,#] Hyeyeon Kang,[†,#] Patrick Y. Yee,[†] Zongwu Fan,[†] Steven A. Hawks,[‡] Laura T. Schelhas,[¶] Selvam Subramaniyan,[§] Ye-Jin Hwang,[∥] Samson A. Jenekhe,[§] Sarah H. Tolbert,[*,†,⊥] and Benjamin J. Schwartz[*,†]

[†]Department of Chemistry and Biochemistry, University of California, Los Angeles, 607 Charles E. Young Drive East, Los Angeles, California 90095-1569, United States

[‡]Lawrence Livermore National Laboratory, 7000 East Avenue, Livermore, California 94550, United States

[¶]SLAC National Accelerator Laboratory, 2575 Sand Hill Road, Menlo Park, California 94025, United States

[§]Department of Chemical Engineering and Department of Chemistry, University of Washington, Seattle, Washington 98195-1750, United States

[∥]Department of Chemical Engineering, Inha University, 100 Inha-ro, Nam-gu, Incheon 22212, South Korea

[⊥]Department of Materials Science and Engineering, University of California, Los Angeles, Los Angeles, California 90095-1595, United States

Supporting Information

ABSTRACT: Bulk heterojunction (BHJ) photovoltaics based on blends of conjugated polymers and fullerenes require an optimized nanoscale morphology. Casting BHJ films using solvent additives such as 1,8-diiodooctane (DIO), 1,8-octanedithiol (ODT), chloronapthalene (CN), or diphenyl ether (DPE) often helps achieve this proper morphology: adding just a few volume percent of additive to the casting solution can improve polymer/fullerene mixing or phase separation, so that solvent additives have become staples in producing high-efficiency BHJ solar cells. The mechanism by which these additives improve BHJ morphology, however, is poorly understood. Here, we investigate how these additives control polymer/fullerene mixing by taking advantage of sequential processing (SqP), in which the polymer is deposited first and then the fullerene is intercalated into the polymer underlayer in a second processing step using a quasi-orthogonal solvent. In this way, SqP isolates the role of the additives' interactions with the polymer and the fullerene. We find using ellipsometry-based swelling measurements that when adding small amounts of low-vapor-pressure solvent additives such as DIO and ODT to solutions of poly(3-hexylthiophene-2,5-diyl) (P3HT), poly[(4,4′-bis(3-(2-ethyl-hexyl)dithieno[3,2-b:″,3′-d]silole)-2,6-diyl-*alt*-(2,5-bis(3-(2-ethyl-hexyl)thiophen-2yl)thiazolo[5,4-*d*]thiazole)] (PSEHTT), or poly[4,8-bis(2-ethylhexyloxy)-benzol[1,2-b:4,5-b′]dithiophene-2,6-diyl-*alt*-4-(2-ethylhexyloxy-1-one)thieno-[3,4-*b*]thiophene-2,6-diyl] (PBDTTT-C), the additives remain in the polymer film, leading to significant swelling. Two-dimensional grazing-incidence wide-angle X-ray scattering measurements show that the swelling is extensive, directly affecting the polymer crystallinity. When we then use SqP and cast phenyl-C_{61}-butyric acid methyl ester (PCBM) onto DIO-swollen polymer films, X-ray photoelectron spectroscopy and neutron reflectometry measurements demonstrate that vertical mixing of the PCBM in additive-swollen polymer films is significantly improved compared with films cast without the additive. Thus, low-vapor-pressure solvent additives function as cosolvent swelling agents or secondary plasticizers, allowing fullerene to mix better into the swollen polymer and enhancing the performance of devices produced by SqP, even when the additive is present only in the polymer layer. DIO and ODT have significantly different fullerene solubilities but swell polymers to a similar extent, demonstrating that swelling, not fullerene solubility, is the key to how such additives improve BHJ morphology. In contrast, higher-vapor-pressure additives such as CN and DPE, which have generally high polymer solubilities, function by a different mechanism, improving polymer crystallinity.

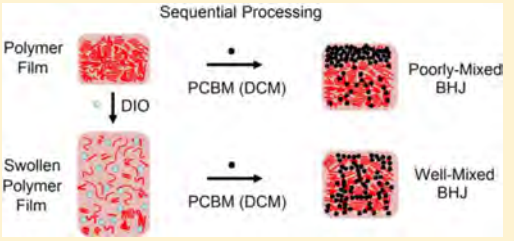

INTRODUCTION

Achieving a high power conversion efficiency (PCE) in organic bulk heterojunction (BHJ) photovoltaics requires forming an ideal nanometer-scale morphology. This morphology must be well-mixed, but also have sufficient phase separation to facilitate contiguous pathways for the different carriers. Most photovoltaics are composed of a blend of a conjugated polymer and a fullerene derivative such as phenyl-C_{61}-butyric

Received: May 2, 2018
Revised: June 21, 2018
Published: July 2, 2018

DOI: 10.1021/acs.jpcc.8b04192
J. Phys. Chem. C XXXX, XXX, XXX−XXX

acid methyl ester (PCBM). Although recent advances have pushed the efficiency of single-junction polymer BHJ solar cells over 14%,[1] attaining the ideal morphology for any given set of conjugated polymer and fullerene materials is quite challenging. In fact, most high-performing materials do not achieve ideal phase separation when they are simply mixed and cast into films, resulting in under-performing devices.[2−5] To address this issue, a variety of techniques have been developed to control polymer/fullerene phase separation, including thermal[6,7] and solvent annealing[8,9] of already-cast BHJ films, changing the host solvent from which the films are cast,[10] and the inclusion of a few volume percent of solvent additives such as 1,8-diiodooctane (DIO), 1,8-octanedithiol (ODT), chloronapthalene (CN), or diphenyl ether (DPE) to the solution from which the films are cast.[2−5,11−17]

Unfortunately, none of these methods for improving BHJ morphology can be effectively utilized to improve device efficiency without significant trial-and-error. For example, thermal annealing improves the morphology for semicrystalline polymers such as poly(3-hexylthiophene-2,5-diyl) (P3HT) and is relatively straightforward in application, but the use of heat tends to degrade the performance of devices based on high-performance push−pull polymers.[18,19] Therefore, thermal annealing is not widely applicable to polymer photovoltaic systems. The use of solvent additives in the casting solution has become perhaps the most widely used approach for tuning BHJ morphology,[2,3] but depending on the polymer used, their effect is highly system specific. One recent report indicates that for multiple polymer/additive systems, the BHJ morphology produced depends sensitively on both the drying kinetics and the way the additives interact with the polymer.[20] In general, BHJ systems that naturally form large polymer and fullerene domains require additives that can improve mixing and decrease domain size,[3−5,14,21,22] while BHJ systems that naturally overmix require additives that can increase phase separation.[3,11,12,16,17] It is not always clear when a particular additive will increase or decrease the average domain size, or how much additive is necessary for optimal performance. This need for trial-and-error is a reflection of the fact that the mechanism by which the additives function is not well understood; indeed, a recent review on the use of additives in BHJ formation calls for additional studies to investigate their method of operation.[2]

In addition to the need for Edisonian optimization, the use of solvent additives is problematic on several other fronts: (1) In general, only very small amounts of additives are required for optimal performance. For example, 3% (v/v) additive is frequently reported as the optimal amount needed for many polymer BHJ systems,[2] while in small-molecule BHJ systems, changes in additive concentration of only 0.35% (v/v) from the optimal concentration can cut device efficiency in half.[23] (2) The optimal amount of additive required frequently changes upon scale-up.[24] Since most additives have high boiling points, they alter the drying kinetics during film-formation, so it is perhaps not surprising that large-scale fabrication methods, which have entirely different drying kinetics than spin-coating in the laboratory, require reoptimization. (3) The most widely used solvent additive, DIO, is both light- and air-reactive, making it of questionable use in any type of future commercial process. Moreover, it is well-known that DIO tends to remain in BHJ films due to its low vapor pressure, requiring extra processing steps to ensure its removal to prevent device degradation upon exposure to light or air.[25−27] (4) Similar to solvent annealing, the time DIO resides within the film can affect the BHJ morphology through "additive annealing", thereby requiring further optimization and kinetic control.[28]

In this work, we focus on the role of the low-vapor-pressure solvent additives DIO and ODT in improving the performance of conjugated polymer/fullerene-based BHJ photovoltaics. DIO has an unusually high PCBM solubility of 120 mg/mL,[29] and because of this, many groups have postulated that the morphology control afforded by DIO is connected with differential solubility of the polymer and fullerene:[4,5,12,22,30] the general idea is that additives help suspend fullerenes in solution for greater periods of time, which in turn affects the fullerene domain size as the film dries. This idea is not consistent, however, with the fact that molecules like ODT, CN, and DPE are also commonly used as additives to favorably improve the BHJ morphology.[11,12,16,20,31,32] ODT has nearly an order of magnitude less fullerene solubility (19 mg/mL for PCBM)[33] than DIO; furthermore, CN and DPE are generally good solvents for most semiconducting polymers and thus afford little differential polymer/fullerene solubility.[34,35] All of this indicates that the mechanism by which additives improve BHJ morphology depends on some property other than differential solubility. For purposes of this work, we classify additives into two categories: low-vapor-pressure additives with poor polymer solubility, such as DIO and ODT, and higher-vapor-pressure additives with generally good polymer solubility, such as CN and DPE. Our primary focus for this paper will be on DIO and ODT, and we will present the case below that additives such as CN and DPE operate by an entirely different mechanism.

In previous work, we presented an alternate method for controlling BHJ morphology and fabricating high-performing solar cells based on a two-step fabrication process called sequential processing (SqP).[7,36,37] In SqP, a film of pure polymer is deposited first, and then the fullerene is intercalated to form a BHJ in a second step by casting from a quasi-orthogonal solvent that swells but does not dissolve the polymer underlayer. To ensure optimal BHJ formation, we showed that the solvent used in the fullerene-casting step must optimally swell the polymer underlayer.[36] This is because swelling lies on the spectrum between no solvent interaction with the polymer and full polymer dissolution. If the fullerene-casting solvent insufficiently swells the polymer, then there will not be good penetration of the fullerene into the polymer to form the requisite BHJ morphology; if the fullerene-casting solvent overswells the polymer, it dissolves some of the polymer film away, again leading to poor BHJ formation. It is also important that the fullerene-casting solvent has a high enough fullerene solubility for mass action to drive fullerene into the properly swollen polymer underlayer.[36,38] We and others have demonstrated that solvent blends can be used to simultaneously optimize both polymer swelling and fullerene solubility, making rational BHJ construction, without the need for significant trial-and-error, tractable via SqP.[36,38] We also have used SqP to infiltrate strong oxidizing agents into films of conjugated polymers to produce highly conductive doped material.[39,40]

In this paper, we take advantage of the fact that SqP decouples the polymer and fullerene components in BHJ formation to investigate the mechanism by which solvent additives improve BHJ morphology. We find that low-vapor-pressure solvent additives function as swelling agents: such

DOI: 10.1021/acs.jpcc.8b04192
J. Phys. Chem. C XXXX, XXX, XXX−XXX

additives alter polymer/fullerene mixing by swelling the polymer film, allowing fullerenes to remain mobile as the BHJ is formed. Our evidence is based on experiments in which we add DIO or ODT to conjugated polymer solutions prior to casting pure polymer films. We observe by spectroscopic ellipsometry that low-vapor-pressure additives such as DIO and ODT remain in the polymer film and significantly swell it, in agreement with previous in situ experiments on polymer/fullerene blend solutions.[20,41−43] We find by grazing-incidence wide-angle X-ray scattering (GIWAXS) that swelling of P3HT films by solvent additives is so great that the polymer crystallinity is significantly altered; this suggests that additives such as DIO and ODT act as "secondary plasticizers",[44] since the additive "plasticizer" primarily enters the amorphous regions of the polymer film. When we then spin-cast PCBM on top of either a pristine or additive-swollen P3HT film in a second SqP step, we find using X-ray photoelectron spectroscopy (XPS) and neutron reflectometry (NR) that the presence of the additive helps to produce complete vertical mixing of P3HT and PCBM into a BHJ, whereas there is significantly less fullerene intercalation when no additive is present in the polymer underlayer. Moreover, the presence of the additive in the polymer underlayer leads to greatly improved sequentially processed device performance. We also show that these same swelling, morphology, and device performance effects involving additives also hold when considering two higher-performing push−pull polymers, poly[(4,4′-bis(3-(2-ethyl-hexyl)dithieno-[3,2-b:″,3′-d]silole)-2,6-diyl-*alt*-(2,5-bis(3-(2-ethyl-hexyl)-thiophen-2yl)thiazolo[5,4-*d*]thiazole)] (PSEHTT)[45] and poly-[4,8-bis(2-ethylhexyloxy)-benzol[1,2-b:4,5-b′]dithiophene-2,6-diyl-*alt*-4-(2-ethylhexyloxy-1-one)thieno[3,4-*b*]thiophene-2,6-diyl] (PBDTTT-C).[46] Therefore, similar to how solvent blends for fullerene solutions can be tuned to optimally swell a polymer film,[36] the primary mechanism of action for low-vapor-pressure solvent additives such as DIO and ODT to improve BHJ morphology is to function as cosolvents that swell conjugated polymer films; in contrast, higher-vapor-pressure additives like CN and DPE work by improving polymer crystallinity. These findings should make it possible to rationally choose solvent additives based on their swelling properties as well as opening additional pathways for BHJ morphology improvement via SqP.

EXPERIMENTAL SECTION

P3HT and PBDTTT-C were purchased commercially, and PSEHTT was synthesized[47] in-house. All other materials used in this study were purchased commercially and were used as received. For polymer-based devices, sequentially processed active layers were prepared by spin-casting a polymer solution onto a PEDOT:PSS-covered substrate. For the P3HT, PSEHTT, and PBDTTT-C solutions, 20, 10, and 10 mg, of polymer, respectively, were dissolved in 1 mL of *o*-dichlorobenzene. The P3HT, PSEHTT, and PBDTTT-C solutions were mixed overnight at 55, 100, and 25 °C, respectively. DIO or ODT (typically 3% by volume) was added directly to the polymer solution prior to heating (if required). The P3HT and PBDTTT-C solutions were cooled to room temperature prior to spin-coating while PSEHTT was spun hot at 100 °C. To remove solvent additives by methanol washing, methanol was deposited on the freshly formed polymer films while the films were still on the spin-coater chuck. Fullerene deposition always occurred within 1 h of casting the polymer film, and no vacuum step was applied between polymer and fullerene spinning to ensure minimal evaporation of any solvent additives between polymer film preparation and fullerene deposition. The detailed procedures of our film and device fabrication are found in the Supporting Information (SI).

Film thicknesses at each stage of the SqP fabrication process were measured by both profilometry and spectroscopic ellipsometry. The latter technique measures the film's refractive index in a nonabsorbing spectral region and constructs a model to fit the data; since the indices of refraction of the films are known, the parameter representing film thickness was varied until the model fit the experimental data.[36,48,49] For the solvent-swelling experiments, each film was placed in a home-built customized vial, which was designed to contain a solvent (e.g., toluene or dichloromethane (DCM)). The film was exposed to the vapor of a swelling solvent in the vial and the thickness monitored until it reached steady-state. In this way, the vial allowed us to perform swelling measurements with solvents such as DCM that were not compatible with the porosimeter instrument. Details of the calibration for the swelling vial and ellipsometry fits can be found in the SI.

X-ray photoelectron spectroscopy (XPS) experiments were performed in-house on Si/active layer films using a Kratos Axis Ultra DLD with a monochromatic Kα radiation source. 2-D GIWAXS experiments were performed at the Stanford Synchrotron Radiation Lightsource on beamline 11-3 using a wavelength of 0.9742 Å. This beamline has a 2-D detector that allows us to integrate the full 2-D data (0−180°), just the in-plane portion of the data (170−180°), and just the out-of-plane portion of the data (100−110°). To ensure minimal additive evaporated between film preparation and the measurement, all films were stored in sealed vials after spin-coating and were prepared less than 24 h from the measurement time. Neutron reflectometry (NR) experiments were performed at Oak Ridge National Laboratory using the Magnetism Reflectometer at the Spallation Neutron Source using a neutron wavelength of 4.41 Å. Scattering length density (SLD) depth profiles were obtained by calculating the reflectivity of a model SLD profile, and iteratively refining the model until the calculated reflectivity profile matched the experimental reflectivity profile. Additional fitting and experimental details can be found in the SI.

Detailed procedures for all other techniques and additional information such as device external quantum efficiency curves, photoluminescence measurements, and so on can be found in the SI and are similar to those published in our previous SqP work.[36,37,50]

RESULTS AND DISCUSSION

Because most organic solar cells are fabricated via blend-casting, in which the polymer or absorbing molecule, fullerene or acceptor molecule, and additive are all mixed together in solution prior to casting the device's active layer, understanding the role of the additive in device morphology and performance is challenging. Many groups have proposed that differential solubility of the fullerene and polymer in the solvent additive is the mechanism by which BHJ morphology and device performance are improved.[4,5,12,22,30] One clue indicating the solvent additive mechanism for device improvement is not differential solubility comes in work performed by Kong et al., in which BHJ films were cast and then a dilute DIO solution was spun onto the BHJ film in a second

DOI: 10.1021/acs.jpcc.8b04192
J. Phys. Chem. C XXXX, XXX, XXX−XXX

processing step.[51] This "post-additive soaking" favorably reorganized the donor and acceptor domains, resulting in significantly improved device efficiencies.[51] Since DIO was added to the film after BHJ formation, this two-step approach indicates the mechanism by which the additive operates is independent of fullerene solubility. Moreover, this work suggests that a fruitful avenue for further investigation into the role of DIO and other solvent additives in BHJ formation would be to form active layers using an alternative fabrication technique.

Exploring the Role of Solvent Additives by Sequential-Processing. Motivated by the work of Kong et al.,[51] we decided to investigate the mechanism by which solvent additives control BHJ morphology using sequential-processing (SqP).[36,37,52] We selected P3HT as the first polymer system to study because of P3HT's semicrystalline nature: this provides a structural handle on the chain spacing and domain orientation via two-dimensional grazing incidence X-ray scattering (GIWAXS), something that is more challenging to characterize with generally more amorphous push−pull polymers. Furthermore, P3HT also provides the advantage of having generally weaker interactions with organic solvents (i.e., poorer solubility) than the push−pull polymers we explore below. Because of this weaker interaction, when depositing PCBM onto a P3HT film by SqP using DCM as the fullerene solvent, DCM's marginal swelling of the polymer underlayer promotes formation of a quasi-bilayer with a fullerene-enriched top surface, which is a highly non-ideal BHJ morphology. This quasi-bilayer structure, however, does provide an opportunity to demonstrate that the BHJ morphology can be improved by DIO due to improved polymer swelling:[36,38] we will show using three polymer systems of varying crystallinity (P3HT, PSEHTT, and PBDTTT-C) that when the fullerene solvent in SqP provides insufficient swelling, the presence of a solvent additive swelling agent in the polymer underlayer converts a non-working system into a working system. Moreover, the extent of the improvement is dependent upon the degree of swelling by the fullerene solvent: if the fullerene solvent promotes near-optimum swelling, the effect of the solvent additive is marginal. Thus, decoupling swelling by solvent additives and swelling by the fullerene solvent allows us to identify swelling as the mechanism for BHJ morphology improvement by solvent additives.

We started by fabricating P3HT/PCBM solar cells using SqP, but with the addition of DIO to the P3HT solution. Since the first step in SqP involves spin-casting a pure polymer film, this decouples the action of DIO from the presence of PCBM, which is added in a second processing step cast from DCM. Figure 1 shows the $J-V$ characteristics of sequentially processed BHJ devices with 0, 3, and 7% (v/v) DIO added to the P3HT solution used in the first SqP step. All devices were measured under AM-1.5 solar illumination, and the plotted data are the average of approximately nine separate devices. Detailed $J-V$ parameters for each set of devices are presented in Table 1. The corresponding EQE spectra for 0, 3, and 7% (v/v) DIO are presented in Figure S1 and additional device conditions (blend-cast devices and annealing) are presented in the Table S1 of the SI. Additional device physics such as dark $J-V$ curve analysis and dark charge extraction by linearly increasing voltage (CELIV) measurements are also described in the SI.

Figure 1 and Table 1 show that without DIO, the currents of the sequentially processed devices are quite low, but that the currents increase significantly with increasing percent DIO added to the polymer solution in the first SqP step. This strongly suggests the DIO−P3HT interaction is responsible for device improvement. Since DIO has a very low vapor pressure,[53] DIO remains in the films prior to the second SqP step where the fullerene is deposited. In fact, the tendency of DIO to remain in BHJ films is known to lower device efficiencies due to its deleterious chemistry in the presence of light or air. To counter the detrimental effects of DIO remaining in BHJ films, several groups have used methanol washing, where pure methanol is spun onto the film to remove the remaining DIO without dissolving the polymer and/or fullerene.[25,26,54] Thus, to investigate whether or not the improvement in device performance was due to DIO remaining in our pure P3HT films, we performed methanol-washing experiments in which we performed the washing step directly after P3HT film formation and prior to PCBM spin-coating. When DIO is removed from the polymer film by methanol washing, we find that the device currents decrease, although not to the same extent as when no DIO was initially present. Furthermore, both methanol-washed devices have almost identical currents. This suggests that similar residual concentrations of DIO remain in the film after methanol washing, regardless of the initial volume percentage of DIO used in casting the polymer film.

The data in Figure 1 also show that although the use of DIO produces the best $J-V$ characteristic, the use of ODT as a

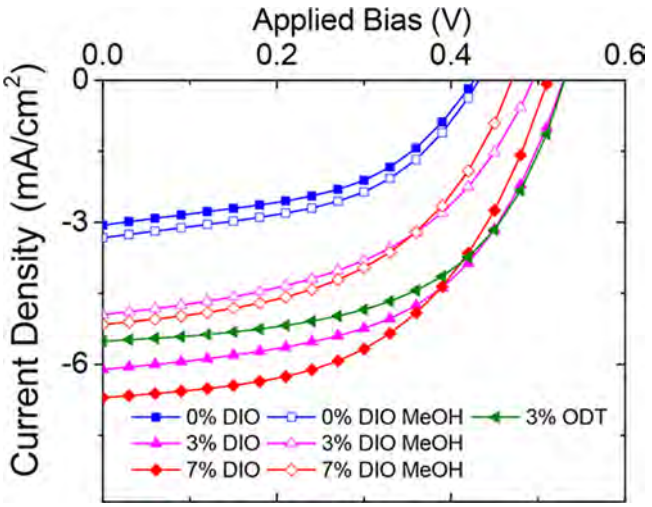

Figure 1. $J-V$ measurements for sequentially processed ITO/PEDOT:PSS/P3HT(DIO)/PCBM/Ca/Al solar cells under AM-1.5 illumination, illustrating the effect of different concentrations of DIO or ODT and subsequent methanol washing on device performance. The filled symbols show that devices fabricated with 0% (v/v) DIO (blue squares), 3% (v/v) DIO (magenta up-triangles), 7% (v/v) DIO (red diamonds), and 3% (v/v) ODT (green left-triangles) in the polymer solution have improved performance with increasing DIO concentration. By contrast, devices in which the polymer films from the first SqP step was methanol-washed prior to deposition of the PCBM (open symbols) show reduced performance compared to unwashed films: 0% (v/v) DIO (hollow blue squares), 3% (v/v) DIO (hollow magenta up-triangles), and 7% (v/v) DIO (hollow red diamonds). Comparison of the 3% DIO and 3% ODT $J-V$ curves shows that both DIO and ODT enhance SqP device performance to a similar extent, and the methanol data suggest that the application of a methanol wash prior to casting the fullerene leaves a similar amount of residual additive in the polymer film, regardless of the initial additive concentration.

DOI: 10.1021/acs.jpcc.8b04192
J. Phys. Chem. C XXXX, XXX, XXX−XXX

Table 1. Summary of P3HT, PSEHTT, and PBDTTT-C Device Parameters

polymer	device condition	V_{oc} (V)	J_{sc} (mA/cm^2)	FF (%)	PCE (%)
P3HT	0% cosolvent SqP	0.422 ± 0.026	3.10 ± 0.16	48.16 ± 3.88	0.63 ± 0.10
	0% cosolvent MeOH SqP	0.430 ± 0.021	3.32 ± 0.11	49.82 ± 4.58	0.71 ± 0.08
	3% DIO SqP	0.531 ± 0.006	6.11 ± 0.29	53.58 ± 2.69	1.74 ± 0.15
	3% DIO MeOH SqP	0.495 ± 0.09	4.95 ± 0.15	47.72 ± 1.05	1.17 ± 0.06
	7% DIO SqP	0.511 ± 0.007	7.15 ± 0.27	50.34 ± 1.32	1.84 ± 0.14
	7% DIO MeOH SqP	0.475 ± 0.017	5.16 ± 0.48	48.78 ± 2.51	1.20 ± 0.13
	3% ODT SqP	0.531 ± 0.011	5.51 ± 0.28	55.06 ± 1.11	1.65 ± 0.19
PSEHTT	0% cosolvent BC	0.700 ± 0.005	10.73 ± 0.27	65.10 ± 3.01	4.89 ± 0.31
	0% cosolvent SqP	0.725 ± 0.003	7.41 ± 0.10	62.99 ± 1.11	3.38 ± 0.04
	3% DIO SqP	0.677 ± 0.004	10.67 ± 0.34	57.06 ± 0.31	4.13 ± 0.14
	7% DIO SqP	0.677 ± 0.005	9.33 ± 0.42	55.71 ± 0.74	3.51 ± 0.10
PBDTTT-C	0% cosolvent BC	0.788 ± 0.001	10.88 ± 0.26	49.40 ± 0.57	4.24 ± 0.08
	0% cosolvent SqP	0.734 ± 0.004	12.36 ± 0.70	52.97 ± 1.06	4.81 ± 0.27
	3% cosolvent BC	0.727 ± 0.002	12.96 ± 0.37	58.60 ± 1.09	5.52 ± 0.14
	3% DIO SqP	0.736 ± 0.002	12.88 ± 0.34	56.34 ± 1.12	5.33 ± 0.05

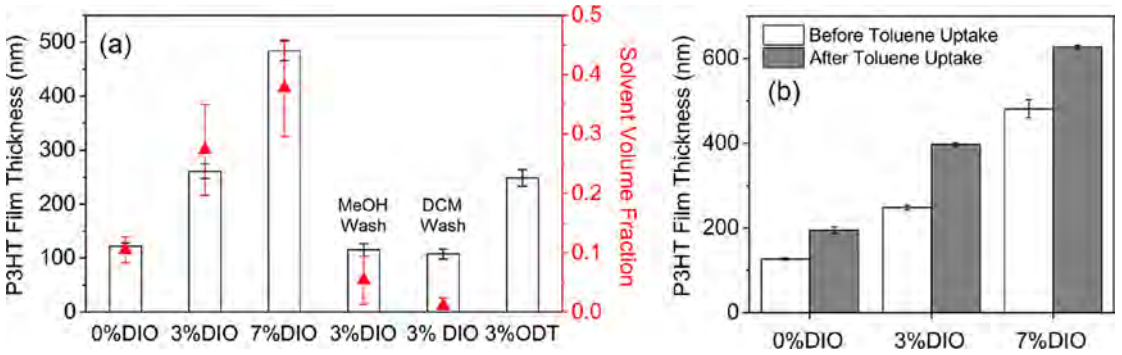

Figure 2. (a) Thickness (bar heights) of pure P3HT films obtained by spectroscopic ellipsometry. The thickness was measured directly after spin-casting for pure P3HT films cast from ODCB with no DIO, 3% (v/v) DIO, 7% (v/v) DIO, 3% (v/v) DIO followed by methanol washing, 3% (v/v) DIO followed by dichloromethane washing, and 3% (v/v) ODT. Adding DIO or ODT and increasing the additive concentration produces thicker polymer films. Washing with methanol or DCM reduces the film thickness to close to the point where no additive was used. The red triangles show effective medium approximation fits to the ellipsometry data that yield the solvent volume fraction in the film (which could be either ODCB or DIO, which have similar refractive index profiles). (b) Thickness of P3HT films cast with 0% (v/v) DIO, 3% (v/v) DIO, and 7% (v/v) DIO before toluene vapor uptake (white bar heights) and after toluene vapor uptake (gray bar heights). The additional swelling by toluene vapor for films with DIO demonstrates DIO's ability to increase the swelling range for P3HT. The error bars represent one standard deviation obtained from averaging over at least three different polymer films.

solvent additive leads to comparably good sequentially processed device performance. Indeed, blend-cast P3HT:PCBM photovoltaics fabricated with DIO and ODT also have similar device characteristics (see SI). This suggests DIO and ODT have a similar interaction with P3HT and work via a similar mechanism of operation. Moreover, we also see similar improvements in sequentially processed device performance with the addition of DIO to films of different push−pull polymers, discussed further below. This leads to the principle lines of inquiry of this paper: for sequentially processed polymer/fullerene photovoltaics, why do DIO and ODT significantly improve device performance? And how does what we learn from devices produced by SqP translate to the broader spectrum of BHJ solar cells fabricated using solvent additives via other processing techniques? In the following sections, we present a series of structural and device measurements on a variety of materials to answer these questions and present a clear mechanism—swelling—by which low-vapor-pressure solvent additives alter BHJ morphology and thus photovoltaic device performance.

Effect of DIO and ODT on P3HT Swelling and Crystallinity. How do low-vapor-pressure solvent additives affect the quality of BHJ solar cells produced by SqP when the additive is used before any fullerene is intercalated into the device? In this section, we first examine the swelling properties of low-vapor-pressure solvent additives on pure P3HT films, and we then explore the changes such additives make in the structure of pure polymer films using X-ray diffraction.

Swelling Properties of Solvent Additives. In previous work, we demonstrated that polymer swelling is responsible for BHJ morphology control in devices produced via SqP.[36] Furthermore, the degree of polymer swelling is critical for optimal device performance. We showed using spectroscopic ellipsometry that the degree of solvent/polymer interaction can be quantified by the Flory−Huggins χ parameter, and that there is an optimal χ to produce the best sequentially processed devices.[36] We also found that we could use solvent blends to simultaneously tune χ and maintain enough fullerene solubility to provide sufficient mass action for fullerene intercalation into the sequentially processed BHJ.[36]

With the idea that optimal solvent swelling is the key to fabricating good sequentially processed BHJ solar cells, we turn next to investigate the role of DIO and ODT in modifying swelling behavior using spectroscopic ellipsometry. For all our

DOI: 10.1021/acs.jpcc.8b04192
J. Phys. Chem. C XXXX, XXX, XXX−XXX

ellipsometry experiments, the various conjugated polymers were spun onto single-crystal Si substrates from solutions of 1,2-dichlorobenzene (ODCB) with or without a small percentage of low-vapor-pressure solvent additive. The height of the bars in Figure 2 show the ellipsometrically determined thicknesses of P3HT films cast from ODCB with and without varying small amounts of solvent additives. Depending on the additive used, there is a substantial difference in thickness of the resulting films. Films cast with additive present are significantly thicker than control films with no additive; for example, the film cast using 7% DIO is nearly 4 times thicker than the film cast from pure ODCB under otherwise identical conditions. The enhancement in film thickness with solvent additives is also general to push-pull polymers, as we discuss in more detail below.

The most logical hypothesis for the increased thickness of the P3HT films cast using DIO and ODT is that these additives remain in the film after the ODCB has evaporated, leaving a polymer film that is highly swollen. Indeed, at 25 °C, the vapor pressure of DIO is 0.04 Pa;[53] that of ODT is 1.60 Pa;[55] while the vapor pressure of ODCB is 181 Pa.[56] The fact that DIO remains in the film longer than higher-vapor-pressure solvents recently has been confirmed by in situ GIWAXS measurements that demonstrated that DIO remains in polymer films for prolonged periods of time.[20,41] This is why low-vapor-pressure additives need to be removed prior to device fabrication (because otherwise they remain in the active layer). When we wash our P3HT films with methanol, we see their thickness returns to within 10% of that obtained for films cast from pure ODCB (the slight increase in remaining thickness is consistent with the idea discussed above that methanol does not fully remove DIO from the film,[25] leaving the films slightly swollen). The device data above suggests that ODT acts in a similar manner to DIO, but with a slightly smaller overall effect; this makes sense in light of ODT's higher vapor pressure, which likely leaves less residual additive in the film relative to DIO.

In addition to inferring the presence of low-vapor-pressure solvent additives in our films by the increase in polymer film thickness, we also can use spectroscopic ellipsometry to directly quantify the amount of additive that remains in the polymer film. To do this, we applied the effective medium approximation (EMA), which states that the refractive index of a mixture is the volume-weighted average of the refractive indices of each of the components.[57] Because we know the wavelength-dependent indices of refraction of both P3HT and DIO, we can use the ellipsometrically measured index of refraction to quantify the DIO volume fraction in each film.[36] The details of our EMA fitting procedure are given in the SI. The DIO volume fractions we obtain are 27% and 36% for the P3HT films cast with 3% (v/v) and 7% (v/v) DIO, respectively, and the DIO volume fraction drops to less than 5% after methanol washing; the data are plotted as the red triangles in Figure 2. Since the DIO volume fraction scales directly with the film thickness, it makes sense that the thickness change is attributed to swelling of P3HT by the residual solvent additive: with such a low vapor pressure, significant amounts of DIO remain in the film and are responsible for the thickness increase.

The residual DIO in P3HT films not only is mostly removed by washing with methanol, but it is also removed by washing with dichloromethane, the solvent we employ to cast the fullerene in our second sequential-processing step. Figure 2 shows that for a P3HT film cast from a 3% (v/v) DIO solution in ODCB, washing with DCM reduces the P3HT film thickness to a value similar to that achieved through methanol washing. Moreover, the ellipsometrically determined residual DIO volume fraction remaining in the film after methanol washing is 5%, while that following DCM washing is only 1%. Thus, DCM more effectively removes DIO from the film than methanol. As a result, when fabricating sequentially processed BHJs, the second casting process combines additive removal and fullerene incorporation into a single step, thereby removing the need for a subsequent separate washing step. This suggests that not only is SqP a tractable route for controlling BHJ morphology, but that it also allows for the use of low-vapor-pressure solvent additives, with all their advantages, without the need for additional processing steps. Finally, the fact that methanol-washed sequentially processed devices perform better than the additive-free devices is

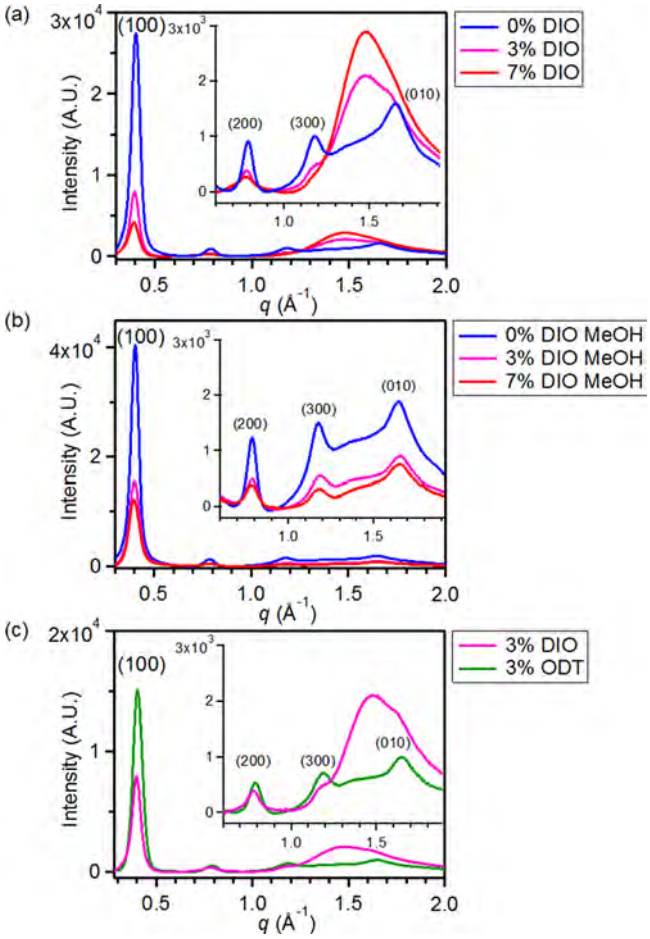

Figure 3. 2-D GIWAXS data for P3HT films cast with and without solvent additives and with and without being subsequently washed with methanol. (a) P3HT films cast with 0% (v/v) additive (blue), 3% (v/v) DIO (purple), and 7% (v/v) DIO (red). (b) Methanol-washed films of P3HT cast with 0% (v/v) additive (blue), 3% (v/v) DIO (purple), and 7% (v/v) DIO (red). (c) P3HT films cast with 3% (v/v) DIO (purple) (same as panel (a)) and 3% (v/v) ODT (green). The inset in each panel shows the high-q π-stacking region on an expanded vertical scale. As the volume percentage of DIO increases, residual DIO inhibits P3HT crystallization. Upon methanol washing, the P3HT crystallinity and orientation are partially restored; restoration is only partial due to incomplete removal of the additive by methanol.

DOI: 10.1021/acs.jpcc.8b04192
J. Phys. Chem. C XXXX, XXX, XXX−XXX

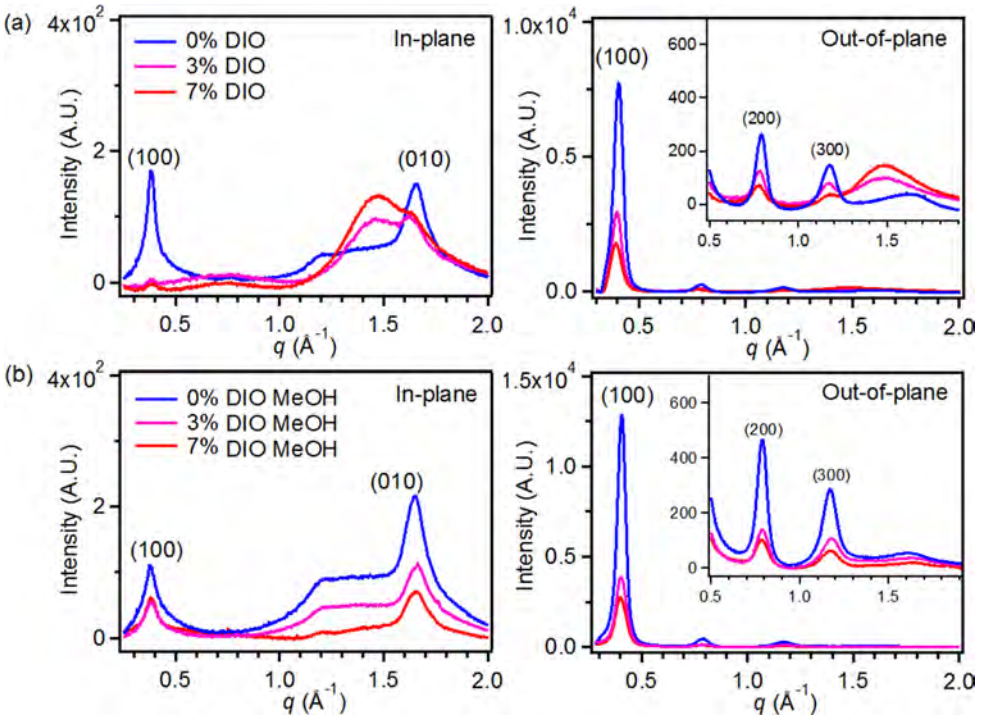

Figure 4. In-plane and out-of-plane integrated portion of the full 2D-GIWAXS from P3HT films cast under different conditions. (a) In-plane (left) and out-of-plane (right) integrated scattering from P3HT films with 0% (v/v) additive (blue), 3% (v/v) DIO (purple), and 7% (v/v) DIO (red). (b) In-plane (left) and out-of-plane (right) integrated 2D-GIWAXS on P3HT films washed with methanol. The insets show the high-q region on an expanded vertical scale. The data indicate that crystalline domains, those that show strong (100) scattering when DIO is added to the film, maintain the standard P3HT edge-on orientation, but that the DIO-swollen regions, indicated by the shifted (010) peak, are more isotropically oriented. When the samples are washed with MeOH, it is possible to recover a significant fraction of the texturing and edge-on orientation of the (010) peaks (Table 3).

consistent with the idea that the residual DIO volume fraction of 5% still provides enough swelling to improve fullerene incorporation and device performance.

In addition to the fact that residual low-vapor-pressure solvent additives are left behind after casting swell a polymer film, we also see that they increase a film's swellability by other solvents. In Figure 2b, we examine how polymer films with different amounts of additive swell upon exposure to toluene vapor. Toluene strongly interacts with P3HT, and P3HT films cast with no solvent additive are swollen by toluene from a thickness of 127 to 194 nm for an effective thickness increase due to toluene-swelling of 67 nm. When P3HT films containing the same thickness of polymer are cast using solvent additives, however, the thickness increase upon swelling with toluene is even larger: P3HT films cast from 3% (v/v) and 7% (v/v) DIO solutions swell from 250 to 397 nm and 482 to 627 nm, respectively, yielding a ∼150 nm increase in film thickness due to toluene uptake. Thus, the presence of DIO not only swells the polymer film, but also increases the swellability by other solvents. This means that solvent additives modify how polymer films interact with other solvents, providing yet another way to tune the Flory–Huggins χ parameter for optimal BHJ formation by SqP.[36]

How Low-Vapor-Pressure Solvent Additives Affect Polymer Crystallinity. As discussed in the previous section, we have established that conjugated polymer films processed using additives such as DIO and ODT are both highly swollen and have increased swellability. It is well-known that polymer crystallinity strongly affects swelling because solvent molecules cannot penetrate into highly crystalline regions.[36,40,58,59] To investigate the swelling effects of solvent additives on the structure of pure P3HT films we performed a series of two-dimensional (2-D) grazing incidence wide-angle X-ray scattering (GIWAXS) experiments. Figure 3a shows integrated diffraction patterns of different P3HT films; the lamellar (100) and $\pi-\pi$ stacking (010) peaks lie at q = 0.4 and 1.6 Å^{-1}, respectively. P3HT is well-known to have an edge-on orientation of the crystallites, showing greater intensity for the (100) diffraction peak in the out-of-plane direction and greater (010) peak intensity in the in-plane directions, as shown in Figure 4. Table 2 summarizes the integrated (100) peak area, which is a measure of relative film crystallinity, for each of the P3HT films that we studied.

Figure 3 and Table 2 show that when P3HT films are cast with DIO or ODT as an additive, the thickness-normalized (100) peak area decreases significantly, indicating that these additives inhibit P3HT crystallinity through polymer swelling, and that higher concentrations of additives lead to lower (100)

Table 2. Integrated (100) Peak Areas for P3HT Films Whose GIWAXS Is Shown in Figure 3

film condition	(100) peak area (A.U.)
P3HT	1621
3% DIO	482
7% DIO	295
P3HT MeOH	2213
3% DIO MeOH	1069
7% DIO MeOH	842
3% ODT	942

DOI: 10.1021/acs.jpcc.8b04192
J. Phys. Chem. C XXXX, XXX, XXX−XXX

peak areas. This is consistent with the thickness measurements shown in Figure 2. Figure 3a also shows that swelling by DIO significantly disrupts the P3HT $\pi-\pi$ stacking: the (010) $\pi-\pi$ stacking peak is shifted to lower q, corresponding to an increase in d-spacing from 3.8 Å with no solvent additive to 4.3 Å when the film is spun with 7% (v/v) DIO. In addition, the width of the (010) peak increases substantially in the presence of swelling solvent additives, indicative of a disordered $\pi-\pi$ stacking network with a wide d-spacing distribution.

Figure 4 shows the in-plane and out-of-plane portions of the integrated GIWAXS from the various P3HT films. As mentioned above, P3HT is well-known to show edge-on polymer chain alignment, with strong (100) lamellar scattering in the out-of-plane direction and strong $\pi-\pi$ (010) scattering in the in-plane direction; the blue curves in Figure 4 for P3HT films with no solvent additive reproduce this known trend. When DIO is added to the solutions from which the films are cast, the data in Figure 4a again indicate that the total crystallinity decreases, as discussed above. However, the crystalline fraction of the sample that remains actually becomes increasingly edge-on oriented as the DIO concentration increases, as indicated by the nearly complete loss of the in-plane (100) diffraction peak in the more highly DIO-swollen samples. This suggests that nonedge-on domains may be less stabilized by the substrate and thus are more easily swelled by DIO. In contrast to the (100) peak, the disordered $\pi-\pi$ (010) peak observed below $q = 1.5$ Å^{-1} is more much isotropic in the DIO-swollen films, reflecting the structure of the swollen fraction of the sample. Figure 4b also shows that methanol washing recovers most of the standard orientational distribution of the P3HT chains, although the previously swollen-and-washed films still show more isotropic scattering than films that never contained the solvent additive; this is quantified in Table 3. Overall, although a number of factors can modify diffraction peak intensity, the observed decrease in domain orientation is clearly associated with swelling.

Table 3. Integrated Out-of-Plane to In-Plane Peak Area Ratio from 2-D GIWAXS for the (100) and (010) Peaks in the P3HT Films after Methanol Washing

	$A_{\text{out-of-plane}}/A_{\text{in-plane}}$	
film condition	(100)	(010)
P3HT (no DIO) MeOH wash	95.8	2.6
P3HT 3% DIO MeOH wash	55.8	2.7
P3HT 7% DIO MeOH wash	43.9	1.1

Figure 3c and Table 2 also compare the structures of P3HT films cast using 3% v/v DIO and ODT to that of a P3HT film cast with no solvent additive. The data show that the films cast with DIO as the additive have the smallest (100) peak area, and thus the lowest crystallinity. This fits well with the swelling measurements discussed above, reflecting the fact that DIO's vapor pressure is lower than that of ODT, so that more DIO remains in the polymer film to inhibit crystallization by swelling. Finally, as also discussed above, Figure 3b and Table 2 show that washing P3HT with methanol removes most residual low-vapor-pressure solvent additive from the films, as measured by both the integrated (100) peak intensity and the return of the (010) peak to its original q position. Table 3 shows that although the methanol-washed P3HT films with solvent additives have restored edge-on orientation, the P3HT chains in the washed films are still somewhat less oriented compared to P3HT films cast without any solvent additive. This is also consistent with literature work demonstrating that methanol washing does not completely remove DIO from polymer films,[25] as verified by our ellipsometry measurements in Figure 2.

Improved Fullerene Mixing and Crystallinity in P3HT/PCBM BHJs with Low-Vapor-Pressure Solvent Additives. Now that we understand the role that low-vapor-pressure solvent additives play in the swelling and reduced crystallinity of pure polymer films, we next consider how solvent additives improve the morphology and performance of bulk heterojunction solar cells produced by SqP, as seen in Figure 1. We first use X-ray diffraction to examine how the presence of DIO affects the structure of sequentially processed BHJ active layers, and then we use optical spectroscopy, X-ray photoelectron spectroscopy, and neutron reflectometry to explore how this additive promotes mixing of fullerenes throughout the polymer underlayer.

How Solvent Additives Affect Sequentially-Processed BHJ Morphology. Figure 5 and Table 4 show the grazing incidence X-ray diffraction of the sequentially processed P3HT/PCBM active layers used for the devices shown in Figure 1. Unlike what we saw with the pure P3HT layers in Figure 3, where the presence of solvent additives made the polymer less crystalline, we see that with BHJ films, the P3HT (100) and (010) peaks become more intense with increasing amounts of DIO or ODT. Much of this increase follows from washing the low-vapor-pressure solvent additive out of the P3HT underlayer when dichloromethane is used to cast the PCBM overlayer in the second SqP step. In addition, for PCBM cast onto P3HT films that are swollen with additive, the solidification process takes longer due to the additives' low vapor pressure. In combination, these two effects cause the improved crystallinity for SqP-based BHJs that used solvent additives. This observation is in agreement with previous studies on blend-cast BHJ films cast with solvent additives.[42,43]

Figure 5 shows that the integrated area of the PCBM diffraction peak at $q \approx 1.4$ Å^{-1} also increases with the presence of low-vapor-pressure solvent additives in the polymer underlayer. We believe the increased fullerene scattering results from increased intercalation of fullerene into the film. PCBM is known to preferentially penetrate into amorphous regions of polymer films during SqP while leaving the crystalline polymer regions intact.[60] Since solvent additives like DIO and ODT lower the overall polymer crystallinity, this offers increased opportunities for PCBM diffusion into the films during SqP, as we document below in the next section. Furthermore, the enhanced mobility of fullerenes within the additive-swollen polymer layer could also lead to enhanced PCBM scattering.

Finally, the data in Figure 5 also show that DIO enhances the scattering from both P3HT and PCBM in the sequentially processed BHJs better than ODT. As discussed above, additives like DIO with lower vapor pressures remain in the film longer and thus increase fullerene diffusion into the film and extend the film-solidification time relative to slightly higher vapor-pressure additives like ODT. Clearly, swelling additives with the lowest vapor pressures will yield the most crystalline materials and the highest fullerene fractions in BHJs produced by SqP.

How Solvent Additives Improve Mixing in Sequentially-Processed BHJs. Given all the evidence we have presented showing that low-vapor-pressure solvent additives remain in

DOI: 10.1021/acs.jpcc.8b04192
J. Phys. Chem. C XXXX, XXX, XXX−XXX

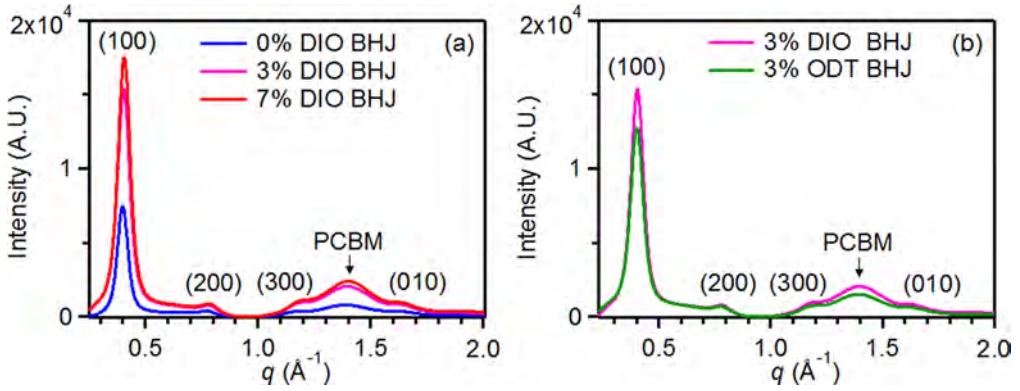

Figure 5. 2-D GIWAXS data for SqP-based P3HT:PCBM BHJs cast with (a) no solvent additive (blue) 3% DIO (purple), and 7% DIO (red). (b) 2-D GIWAXS data for SqP-based P3HT:PCBM BHJs cast with 3% DIO (same as panel (a)) and 3% ODT (green). As the % (v/v) DIO increases, the lower vapor pressure DIO increases the film-solidification time, which improves P3HT crystallinity. ODT, with its higher vapor pressure, evaporates faster and produces a less crystalline film.

Table 4. Integrated (100) Peak Areas for the Sequentially-Processed P3HT/PCBM BHJs Whose GIWAXS Is Shown in Figure 5

P3HT:PCBM BHJ film condition	(100) peak area (A.U.)
0% DIO	315
3% DIO	720
7% DIO	829
3% ODT	649

the polymer film and swell it, the final question we need to address is how such additives affect the mixing and structure of the fullerene intercalated into the polymer following SqP. The easiest place to start is to examine the amount of fullerene that penetrates into the polymer underlayer in the second SqP step with and without additives present in the polymer film. Unfortunately, the UV−visible absorption spectrum of a P3HT/PCBM BHJ film does not provide an accurate way to quantify the polymer/fullerene ratio because the P3HT absorption spectrum and cross-section in the film are highly sensitive to the degree of polymer crystallinity; instead, we have shown that the polymer/fullerene ratio can be accurately determined by redissolving the cast BHJ films and quantifying the ratio of polymer to fullerene using UV−vis spectroscopy of the resultant solution.[37] Using this redissolution method, which is shown in more detail in Figure S3 of the SI, we find that the PCBM:P3HT mass ratios in sequentially processed BHJs where the polymer layer was cast with 0, 3, and 7% (v/v) DIO were 0.80, 0.80, and 0.92, respectively. This shows that in addition to mass action[37] and fullerene solvent selection,[36,38] the degree of swelling/swellability of the polymer underlayer plays a critical role in controlling the fullerene loading in SqP.

Given that more fullerene enters the polymer films when low-vapor-pressure solvent additives are present, the next question we address is how those fullerenes are distributed throughout BHJs produced by SqP. First, we probed the composition at the top surface of our sequentially processed BHJs using X-ray photoelectron spectroscopy (XPS). XPS provides a sensitive measure of composition at the top surface by measuring the sulfur-to-carbon (S/C) ratio; this is because PCBM does not contain sulfur but P3HT does.[61−63] We determined this ratio by fitting the measured sulfur 2p and carbon 1s spectral lines (see the SI for experimental and analysis details); a higher S/C ratio indicates a lower amount of fullerene at the top surface of the BHJ film and vice versa.

Figure 6a shows that for a pure P3HT film, the surface composition is about 6.7% sulfur. When PCBM is spun on top of a pure P3HT film from DCM, the top-surface sulfur-to-carbon ratio drops to 0.8%, indicating that most of the top surface of the film is covered with non-sulfur-containing

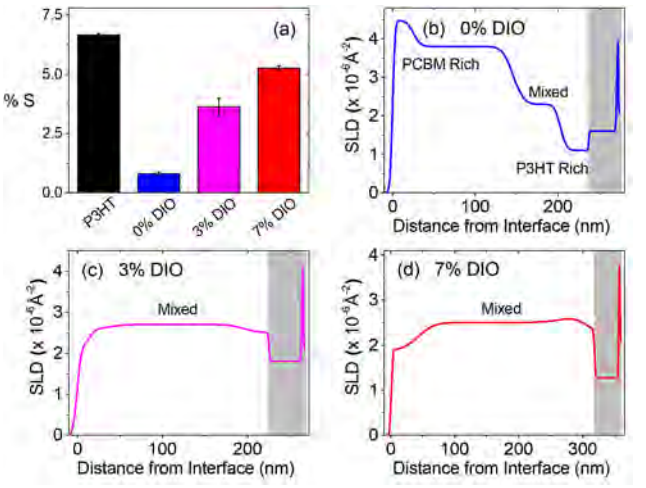

Figure 6. (a) Top-surface sulfur-to-carbon (S-to-C) composition ratios of sequentially processed P3HT:PCBM BHJ films with 0% DIO (blue), 3% DIO (purple), and 7% DIO (red) as measured by XPS; the S-to-C ratio for a pure P3HT film with no PCBM or solvent additive is shown in black for reference. The decreased S-to-C ratio in the 0% additive BHJ indicates that PCBM covers the top surface of the film. The increase in the S-to-C ratio when solvent additives are present demonstrates increased fullerene intercalation upon swelling. The error bars represent one standard deviation with an average taken over at least three different films. (b−d) Neutron reflectivity (NR) scattering length density (SLD) depth profiles of SqP-based P3HT:PCBM BHJ films obtained by fitting the NR data in Figure S12 for 0% (v/v) DIO (blue, panel b), 3% (v/v) DIO (purple, panel c), and 7% (v/v) DIO (red, panel d). For (b−d), our NR model is constructed from multiple layers of variable thicknesses, ensuring the active-layer/air interface is at the origin, with the underlying PEDOT:PSS/Si interface shown in gray. Both the NR and XPS data show that with increasing amounts of solvent additive present in the polymer film prior to SqP, the surface composition of the BHJ film becomes increasingly depleted in fullerene. The most uniform depth profile with a surface composition closest to the bulk composition is found at the optimal DIO additive concentration of 3% (v/v).

DOI: 10.1021/acs.jpcc.8b04192
J. Phys. Chem. C XXXX, XXX, XXX−XXX

fullerene. This observation is consistent with previous work,[64] and is explained by the fact that DCM is a relatively poor swelling solvent for P3HT, so PCBM cannot uniformly penetrate into the polymer underlayer. This is why sequentially processed P3HT/PCBM devices without solvent additives have poor device efficiencies unless they are subsequently thermally annealed to drive PCBM, which has a higher surface energy than P3HT, toward the high surface energy substrate.[64−66]

In contrast to the fact that SqP leaves fullerene predominantly on top of pure P3HT films, Figure 6a also shows that the presence of DIO in the polymer layer increases the top-surface sulfur-to-carbon ratio. With just 3% (v/v) DIO in the P3HT underlayer, the top surface of the film is significantly enriched with P3HT, having a sulfur composition consistent with the bulk 1:0.8 P3HT:PCBM composition ratio measured by redissolution UV−vis.[37] When we proceed to 7% (v/v) DIO in the polymer film, we see that the surface composition has an even higher percentage of P3HT at the surface, close to that of a pure P3HT film. This shows that a sufficient amount of solvent additive can swell a polymer film so much that it allows the fullerene to be driven completely through the film: the higher-surface energy PCBM has enough vertical mobility through the swollen film to fully avoid the energetically unfavorable top interface, as has been observed in films of other conjugated polymers in previous work.[67] This increased diffusion of PCBM is consistent with solvent additives such as DIO and ODT acting as plasticizers for the polymer (see SI).

To further characterize the extent of fullerene penetration through the entire BHJ film thickness, we also performed a series of neutron reflectometry (NR) experiments. NR serves as an excellent probe of molecular distribution along the direction perpendicular to the plane of the film.[64] The active layers measured were spin-coated onto PEDOT:PSS-coated Si substrates for the measurement. Additional details regarding the experimental procedure and fitting of the data to produce the scattering length density (SLD) profiles can be found in the SI. Interpretation of the SLD profiles is based on the fact that pure P3HT has an SLD of ∼0.8 and pure PCBM has an SLD of ∼4.5, while BHJ mixtures show a weighted average of the two pure SLD values. This contrast allows us to resolve differences between PCBM-rich, P3HT-rich, and mixed regions of the BHJ films.

The SLD profiles in Figures 6b−d show the vertical distribution of P3HT and PCBM throughout the BHJ films; the profiles are in excellent agreement with our XPS results. For BHJs made without solvent additives, a higher SLD value representative of nearly pure PCBM is seen at the top surface, while the bottom of the polymer layer near the substrate contains essentially no fullerene. This is because the DCM solvent used in the second SqP step only weakly swells P3HT,[36,58,60,68] and because the high vapor pressure of DCM at 25 °C (58,000 Pa)[69] limits the time available for fullerene diffusion into the film, resulting in a fullerene-rich top surface.[64,70−72] Nonetheless, there is enough swelling of P3HT and time prior to DCM evaporation to allow some PCBM to intercalate into the upper part polymer network, establishing a limited mixed region.[64,65] This highly nonuniform vertical density of fullerene explains the low device currents seen in Figure 1.

The story clearly changes, however, with DIO present in the polymer underlayer. With 3% (v/v) DIO, the NR SLD profile shows complete fullerene mixing throughout the entire film thickness, with a surface composition that closely matches that of the bulk. This is perfectly consistent with the idea that solvent additives are swelling agents, providing time and space for mass action from the second SqP solution to drive fullerene into the swollen polymer film. When the additive concentration is increased to 7% (v/v) DIO, the SLD profile shows good mixing of P3HT and PCBM, explaining the similar performance of the devices made from 3% and 7% DIO. The 7% DIO SLD profile, however, also shows a slight deficit of PCBM near the top surface, consistent with the XPS data. This is because 7% (v/v) DIO swells P3HT more than 3% (v/v) DIO, allowing PCBM to move away from the top interface due to its higher surface energy.[62]

This picture of changes in mixing with the presence of low-vapor-pressure additives in the polymer underlayer is supported by the decrease in the number of dark carriers seen in each of the various active layers,[37,50] shown in Figure S2 and discussed in more detail in the SI. The SI also shows an analysis of the dark $J-V$ curves for these devices (see Table S1), in which there is increased dark recombination current and a higher ideality factor when solvent additives are present. This is consistent with enhanced mixing caused by additives since smaller domains increases charge recombination. The fact that the unmixed domain size decreases for BHJs cast from DIO or ODT is one of the reasons that when blend casting, many polymer BHJ systems are optimized using binary additive blends consisting of DIO and a higher-vapor-pressure additive such as CN or DPE, which help to maintain domain purity.[73−75] Overall, the XPS and NR results paint a clear and consistent picture: the addition of DIO controls both the vertical mixing and overall morphology of polymer/fullerene bulk heterojunction active layers through swelling of the polymer, and this in turn directly controls device performance.

Generality of Low-Vapor-Pressure Solvent Additives Acting as Swelling Agents: Push−Pull Polymer Systems. Having demonstrated the swelling effect and associated BHJ morphology improvement of solvent additives such as DIO and ODT on the sequentially processed P3HT system, we turn next to exploring the generality of our conclusions for more modern push−pull polymer systems. We note that push−pull polymers, which are generally much more amorphous than P3HT, require the use of binary solvent blends for efficient SqP and are not easily fabricated using a single fullerene solvent via SqP.[36] Finding a single SqP solvent is difficult because these amorphous polymers and fullerenes have similar solubilities in many organic solvents. The use of solvent blends, however, adds complexity to a fundamental study and could possibly mask the role of solvent additives, so we focus here on single-solvent SqP.

Two systems that are amenable to single-solvent SqP with DCM are the higher-efficiency push−pull polymers PSEHTT[45] and PBDTTT-C.[46] Both of these materials are sufficiently crystalline so as not to dissolve in DCM, allowing us to make a direct comparison to the work on P3HT in the previous sections. For these materials, the relative crystalline order goes as PBDTTT-C < PSEHTT < P3HT. Both PSEHTT and PBDTTT-C are more strongly swollen by DCM than P3HT, so one might expect that solvent additives will have a smaller effect for these systems than for P3HT. In combination, the behaviors we see using this full series of polymers will allow us to understand in detail the general principles of solvent additives functioning by polymer swelling.

DOI: 10.1021/acs.jpcc.8b04192
J. Phys. Chem. C XXXX, XXX, XXX−XXX

Figure 7a shows ellipsometry-based swelling measurements on films of both PSEHTT and PBDTTT-C with and without DIO. The film thicknesses without DIO (blue bars) are quite a bit smaller than those of P3HT, reflective of the fact that optimized BHJ devices of the push−pull polymers require thinner films. The data show clearly that as with P3HT (Figure 2a), the push−pull polymers are significantly swollen by DIO, which clearly remains in the polymer films.

To verify that DIO-induced swelling is indeed what improves device performance with push−pull polymer systems, we fabricated PSEHTT and PBDTTT-C BHJ devices by SqP using PCBM as the electron acceptor. As shown in Figure 7b, the performance of sequentially processed PSEHTT:PCBM devices matches the trends observed for P3HT: sequentially processed devices without DIO demonstrate a low current, but improve markedly when DIO is added to the polymer underlayer. Even though PSEHTT-based devices fabricated by SqP do not work better than those made by blend-casting in this case (largely because DCM does not have the correct Flory−Huggins χ to optimally swell this polymer), we see that with 3% DIO, the current of the sequentially processed device matches that of the blend-cast device. This indicates that the additional swelling provided by DIO is key to infiltrating fullerene into the device via SqP. We also note that unlike with P3HT, increasing the DIO fraction to 7% leaves the PSEHTT polymer film over-swollen, reducing device efficiency.

Figure 7c compares the performance of blend-cast and sequentially processed photovoltaic devices based on the more amorphous PBDTTT-C polymer combined with PCBM, with and without the use of DIO. Because PBDTTT-C swells extremely well with DCM, the efficiency of the sequentially processed device without DIO is already quite good, and exceeds that of the blend-cast device without DIO. Thus, in the case of PBDTTT-C, DCM acts as an already close-to-optimized SqP solvent: DCM has high fullerene solubility and almost adequate swelling. This means that there is only a marginal improvement to be had by additional swelling with DIO. Indeed, the data show that the sequentially processed device efficiency does improve upon the addition of 3% DIO, but the improvement is more modest than in the case of P3HT or PSEHTT. Interestingly, when DIO is used for this materials combination, the blend-cast and sequentially processed devices have identical efficiencies. This indicates that for PBDTTT-C, the combination of 3% DIO and DCM provides optimal swelling during SqP, leading to a BHJ morphology that is nearly identical to that obtained with blend-casting from ODCB. We note that for all polymer systems studied, 3% DIO is the optimum concentration, consistent with previous polymer−fullerene blend-cast studies that use small fractions of DIO.[16,76,77] Overall, as discussed in the next section, the use of solvent additives can be beneficial with either traditional blend-casting or SqP, but it is important to realize that in the end, additives work by polymer swelling and the optimal amount of polymer swelling varies from one system to the next.

Low-Vapor-Pressure Solvent Additives Are Cosolvent Swelling Agents. We have shown that the mechanism by which low-vapor-pressure solvent additives work to control BHJ morphology is by swelling of conjugated polymer films. This swelling or secondary plasticization[44,78,79] facilitates mixing of the fullerene into the polymer underlayer during the second step of SqP. Thus, low-vapor-pressure solvent additives function as cosolvent swelling agents. DIO and ODT's ability to swell and remain in the polymer film lowers

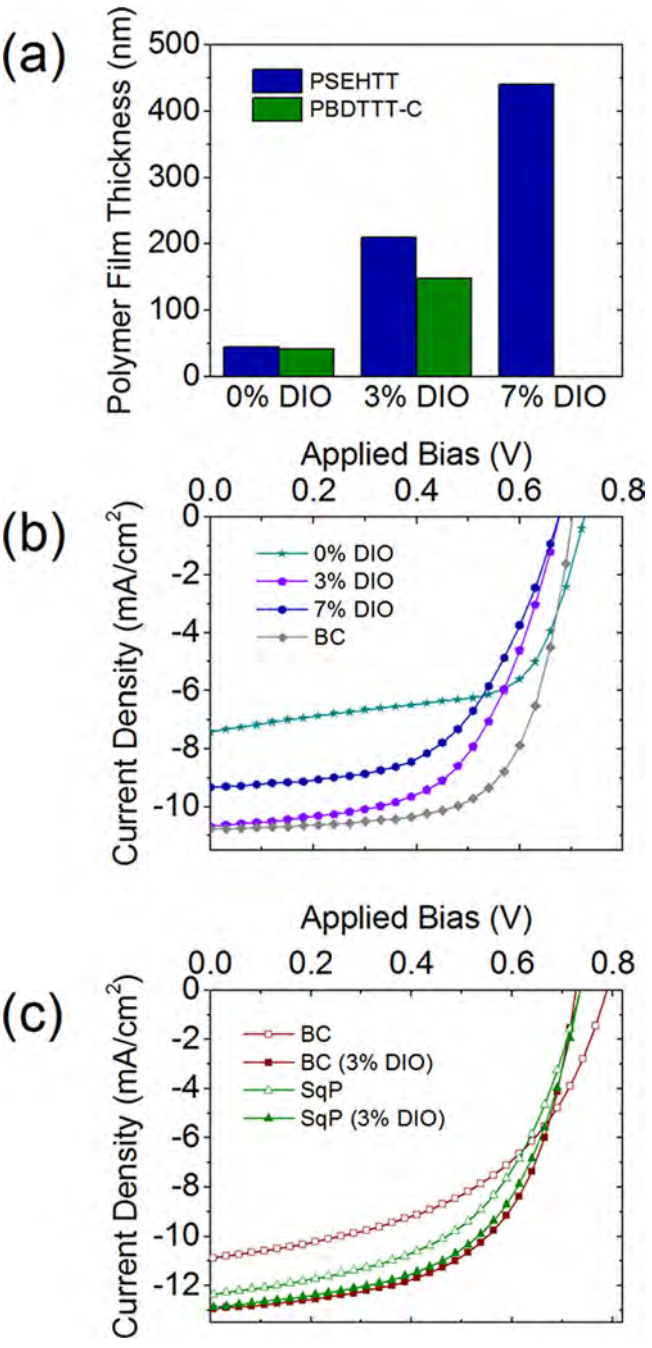

Figure 7. (a) Thickness measurements of PSEHTT (blue) and PBDTTT-C (green) polymer films as measured by spectroscopic ellipsometry. The film thickness is measured for films cast from polymer solutions containing 0% DIO, 3% DIO, and 7% DIO. (b) *J*−*V* curves for PSEHTT:PCBM sequentially processed devices with 0% DIO (teal stars), 3% DIO (violet pentagons), and 7% DIO (navy hexagons). The blend-cast device *J*−*V* data is represented by gray diamonds. (c) *J*−*V* curves for PBDTTT-C:PCBM sequentially processed (green) and blend-cast (maroon) devices without (hollow symbols) and with 3% DIO (filled symbols). The ITO/PEDOT:PSS/Polymer(DIO)/PCBM/Ca/Al solar cells were tested under AM-1.5 illumination and illustrate the effect of different concentrations of DIO for sequentially processed and blend-cast (BC) devices. For both PSEHTT and PBDTTT-C, the device performance for sequentially processed devices increases with 3% DIO and matches or closely matches the blend-cast result. The efficiency increase is due to DIO swelling the polymer film prior to PCBM spin-casting.

DOI: 10.1021/acs.jpcc.8b04192
J. Phys. Chem. C XXXX, XXX, XXX−XXX

the requirement for swelling power in the fullerene-casting solvent used in SqP. Thus, swelling agents/solvent additives function similarly to solvent blends in controlling BHJ morphology by SqP:[36] the main difference is that solvent additives/swelling agents swell the polymer in the initial casting step, whereas solvent blends are designed to swell the film in the second SqP step.

As mentioned in the introduction, we classify solvent additives into two general categories: low-vapor-pressure additives that swell but do not dissolve semiconducting polymers, such as DIO and ODT, and higher-vapor-pressure additives that are generally good polymer solvents, such as CN and DPE. At 25 °C, CN and DPE have vapor pressures of 3.87[80] and 3.00 Pa,[81] respectively, so these additives will evaporate from polymer films much more quickly than additives like DIO and ODT. This means that CN and DPE improve BHJ performance by an entirely different mechanism from DIO and ODT: we believe that their primary function is to act as polymer cosolvents.[35,73,82] The presence of such cosolvents is important for less-crystalline polymers to increase the film solidification time: even though additive cosolvents such as CN and DPE have higher vapor pressures than DIO and ODT, they still have lower vapor pressures than most traditional polymer casting solvents, such as toluene or ODCB. The increased film solidification time offered by the presence of additives like CN and DPE acting as cosolvents facilitates higher polymer crystallinity and domain purity, reducing carrier recombination and increasing mobility. In the SI, we present results for CN that are consistent with this picture. Moreover, recent work has demonstrated that DPE improves the performance of thick BHJs based on PTB7 by increasing polymer crystallinity and therefore charge transport.[32,75] In addition, this idea explains recent work in which a power conversion efficiency of 9.5% was achieved for the PTB7:$PC_{71}BCM$ system using a binary solvent additive blend of DIO and DPE:[75] the efficiency enhancement is attributed to the increased crystallinity afforded by DPE and the increased fullerene dispersion afforded by DIO. Similar improvements also have been reported with other polymer/dual additive combinations, including CN/DIO,[83] CN/ODT,[31] and DPE/DIO.[75] Thus, for many systems, achieving optimal efficiency requires a polymer cosolvent (CN or DPE) to improve phase purity/polymer crystallinity as well as a swelling agent (DIO or ODT) to ensure sufficient mixing of the components between the pure domains.

With the mechanism of action of low-vapor-pressure solvent additives/swelling agents understood, we now have additional routes toward tractable BHJ optimization via SqP. Not only can one swell a polymer film through solvent blends, but one can swell the polymer film during polymer deposition. Indeed, our picture of low-vapor-pressure solvent additives functioning as polymer swelling agents is supported by the post-additive soaking experiments of Kong et al. via their secondary solvent washing procedure. In these experiments, over-phase-separation BHJs are treated with a secondary solvent washing step; this solvent is a mixture of a host solvent and DIO. The authors find that upon this post-additive soak, the BHJ is favorably reorganized, resulting in more ideal phase separation for a preformed BHJ.[51] Our work demonstrates that low-vapor-pressure solvent additives such as DIO act as polymer swelling agents and explains the post-additive soaking effect: by adding DIO to a pre-formed BHJ, DIO swells the polymer film and the extended film-formation time facilitates polymer/fullerene mixing, driven by DIO in the swollen polymer. Thus, solvent additives make BC more SqP-like, as the residual additive swells the polymer film. The fact that Kong et al. report that thicker BHJ films required increased amounts of additive in the post-additive soaking is consistent with our conclusion that DIO acts as a polymer swelling agent, as additional DIO is required to swell more polymer material. Indeed, this idea fits nicely with our results in Figures 2a and 7a, where thin films of PSEHTT and PBDTTT-C required only 3% DIO to swell to approximately four times their initial thickness while P3HT films that were more than twice as thick required 7% DIO to be swelled by the same relative amount.

Although this study focuses primarily on SqP as a way to elucidate the mechanism of action of solvent additives, it also helps explain the role of solvent additives in improving the performance of more traditional blend-cast devices. With the polymer and fullerene codissolved in a binary solution of host solvent and swelling agent/solvent additive, the additive serves to swell the polymer and delay film solidification due to its low vapor pressure. It also serves to drive mixing between the polymer and fullerene; similar to the way that many ternary solvent blends are miscible even when binary pairs of the same solvents are not.[84] In this way, swelling alters the degree of polymer and fullerene mixing and thus favorably controls BHJ domain sizes. This mechanism accounts for the majority of trends reported in the literature for high-performing push−pull polymers which tend to overaggregate,[4,5,14,21,22,51] and also fits well with studies that have observed a significant increase in film formation time when DIO is used during blend-casting.[20,41,85]

CONCLUSIONS

In summary, low-vapor-pressure solvent additives used to improve BHJ morphology in conjugated polymer/fullerene photovoltaics are polymer swelling agents. By fabricating films through sequential-processing and adding swelling agents to the polymer solution, we observed significant structural changes. As verified by spectroscopic ellipsometry, solvent additives such as DIO or ODT swell P3HT, PSEHTT, and PBDTTT-C and remain in polymer films due to their low vapor pressures. The presence of solvent additives also allows non-optimal fullerene solvents in the second SqP step to more effectively swell polymer films. This means that solvents that are less effective at swelling (and thus less likely to dissolve a polymer film) can be utilized as fullerene-casting solvents for SqP in conjunction with solvent additives. A direct example of this is the fact that a poor swelling solvent such as DCM still can provide for good fullerene intercalation and crystallization in SqP when solvent additives are present. Furthermore, DCM removes DIO, thereby including fullerene intercalation and DIO removal into a single step. In summary, the dramatic changes in vertical fullerene distribution observed by XPS and neutron reflectometry upon addition of DIO are a testament to the large changes in molecular diffusivity that can be generated using solvent additives.

Although we isolated the swelling role of additives like DIO and ODT using SqP for three different polymer systems, the fact that such swelling agents have low vapor pressures and remain in the film, providing time and mobility for fullerenes to redistribute, explains their mechanism of operation in traditional blend-casting: low-vapor-pressure additives swell the polymer film, making blend-casting more like sequential-processing, where swelling is the primary mechanism. Overall,

DOI: 10.1021/acs.jpcc.8b04192
J. Phys. Chem. C XXXX, XXX, XXX−XXX

low-vapor-pressure additives like DIO and ODT control BHJ morphology by functioning as secondary plasticizers. Additives such as CN and DPE, which have higher vapor pressures, act more as cosolvents to improve polymer crystallization and domain purity, as discussed in more detail in the SI.

Overall, this work demonstrates the importance of polymer swelling to ensure both good mixing and good crystallinity of polymer donor and fullerene derivative acceptor materials in BHJ photovoltaics. Furthermore, the use of solvent additives in SqP is an approach that is widely applicable to multiple polymer systems as the low-vapor-pressure swelling agent can be added directly to the pure polymer in solution: by directly swelling a polymer film to a precisely controlled degree using simple swelling measurements, it should be possible to find a tractable route toward optimal BHJ formation.

■ ASSOCIATED CONTENT

Supporting Information

The Supporting Information is available free of charge on the ACS Publications website at DOI: 10.1021/acs.jpcc.8b04192.

Details on solar cell materials, photovoltaic device and active layer fabrication procedures, $J-V$ parameters, external quantum efficiency (EQE) measurements, recombination analysis, dark charge extraction by linearly increasing voltage (CELIV) measurements, active-layer composition analysis, UV−visible spectra, spectroscopic ellipsometry experimental apparatus and analysis, grazing incidence wide-angle X-ray scattering (GIWAXS) experiments and analysis, X-ray photoelectron spectroscopy (XPS) experiments and analysis, neutron reflectometry experiments and analysis, photoluminescence (PL) quenching experiments, secondary plasticization, and using chloronaphthalene as a solvent additive (PDF)

■ AUTHOR INFORMATION

Corresponding Authors

*E-mail: tolbert@chem.ucla.edu.
*E-mail: schwartz@chem.ucla.edu.

ORCID

Laura T. Schelhas: 0000-0003-2299-1864
Sarah H. Tolbert: 0000-0001-9969-1582
Benjamin J. Schwartz: 0000-0003-3257-9152

Author Contributions

#M.T.F. and H.Y.K. contributed equally to this work.

Notes

The authors declare no competing financial interest.

■ ACKNOWLEDGMENTS

This work was supported by the National Science Foundation (NSF) under Grant Numbers CBET-1510353 and CHE-1608957. The XPS instrument used in this work was obtained with support from NSF under grant number 0840531. The X-ray diffraction studies presented in this manuscript were carried out at the Stanford Synchrotron Radiation Lightsource. Use of the Stanford Synchrotron Radiation Lightsource, SLAC National Accelerator Laboratory, is supported by the U.S. Department of Energy, Office of Science, Office of Basic Energy Sciences, under Contract DE-AC02-76SF00515. Neutron reflectometry studies made use of the ORNL Spallation Neutron Source, which is supported by the Scientific User Facilities Division, Office of Basic Energy Sciences, U.S. Department of Energy. Contributions from S.A.H. were performed under the auspices of the U.S. Department of Energy by LLNL under Contract DE-AC52-07NA27344. The authors wish to thank Drs. Jordan Aguirre and Guangye Zhang for helpful discussions.

■ REFERENCES

(1) Li, S.; Ye, L.; Zhao, W.; Yan, H.; Yang, B.; Liu, D.; Li, W.; Ade, H.; Hou, J. A Wide Band-Gap Polymer with a Deep HOMO Level Enables 14.2% Efficiency in Polymer Solar Cells. *J. Am. Chem. Soc.* **2018**, *140*, 7159.

(2) Kwon, S.; Kang, H.; Lee, J.-H.; Lee, J.; Hong, S.; Kim, H.; Lee, K. Effect of Processing Additives on Organic Photovoltaics: Recent Progress and Future Prospects. *Adv. Energy Mater.* **2017**, *7*, 1601496.

(3) Liao, H.-C.; Ho, C.-C.; Chang, C.-Y.; Jao, M.-H.; Darling, S. B.; Su, W.-F. Additives for Morphology Control in High-Efficiency Organic Solar Cells. *Mater. Today* **2013**, *16*, 326−336.

(4) Liang, Y.; Xu, Z.; Xia, J.; Tsai, S.-T.; Wu, Y.; Li, G.; Ray, C.; Yu, L. For the Bright Future - Bulk Heterojunction Polymer Solar Cells with Power Conversion Efficiency of 7.4%. *Adv. Mater.* **2010**, *22*, E135−E138.

(5) Zhao, J.; Li, Y.; Yang, G.; Jiang, K.; Lin, H.; Ade, H.; Ma, W.; Yan, H. Efficient Organic Solar Cells Processed from Hydrocarbon Solvents. *Nat. Energy* **2016**, *1*, 15027.

(6) Ma, B. W.; Yang, C.; Gong, X.; Lee, K.; Heeger, A. J. Thermally Stable, Efficient Polymer Solar Cells with Nanoscale Control of the Interpenetrating Network Morphology. *Adv. Funct. Mater.* **2005**, *15*, 1617−1622.

(7) Ayzner, A. L.; Wanger, D. D.; Tassone, C. J.; Tolbert, S. H.; Schwartz, B. J. Room to Improve Conjugated Polymer-Based Solar Cells: Understanding How Thermal Annealing Affects the Fullerene Component of a Bulk Heterojunction Photovoltaic Device. *J. Phys. Chem. C* **2008**, *112*, 18711−18716.

(8) Li, B. G.; Yao, Y.; Yang, H.; Shrotriya, V.; Yang, G.; Yang, Y. "Solvent Annealing" Effect in Polymer Solar Cells Based on Poly(3-hexylthiophene) and Methanofullerenes. *Adv. Funct. Mater.* **2007**, *17*, 1636−1644.

(9) Zhao, Y.; Xie, Z.; Qu, Y.; Geng, Y.; Wang, L. Solvent-Vapor Treatment Induced Performance Enhancement of Poly(3-hexylthiophene): Methanofullerene Bulk-Heterojunction Photovoltaic Cells. *Appl. Phys. Lett.* **2007**, *90*, 043504.

(10) Walker, B.; Tamayo, A.; Duong, D. T.; Dang, X.-D.; Kim, C.; Granstrom, J.; Nguyen, T.-Q. A Systematic Approach to Solvent Selection Based on Cohesive Energy Densities in a Molecular Bulk Heterojunction System. *Adv. Energy Mater.* **2011**, *1*, 221−229.

(11) Peet, J.; Kim, J. Y.; Coates, N. E.; Ma, W. L.; Moses, D.; Heeger, A. J.; Bazan, G. C. Efficiency Enhancement in Low-Bandgap Polymer Solar Cells by Processing with Alkane Dithiols. *Nat. Mater.* **2007**, *6*, 497−500.

(12) Lee, J. K.; Ma, W. L.; Brabec, C. J.; Yuen, J.; Moon, J. S.; Kim, J. Y.; Lee, K.; Bazan, G. C.; Heeger, A. J. Processing Additives for Improved Efficiency from Bulk Heterojunction Solar Cells. *J. Am. Chem. Soc.* **2008**, *130*, 3619−3623.

(13) Coffin, R. C.; Peet, J.; Rogers, J.; Bazan, G. C. Streamlined Microwave-Assisted Preparation of Narrow-Bandgap Conjugated Polymers for High-Performance Bulk Heterojunction Solar Cells. *Nat. Chem.* **2009**, *1*, 657−661.

(14) Guo, X.; Cui, C.; Zhang, M.; Huo, L.; Huang, Y.; Hou, J.; Li, Y. High Efficiency Polymer Solar Cells Based on Poly(3-hexylthiophene)/Indene-C70 Bisadduct with Solvent Additive. *Energy Environ. Sci.* **2012**, *5*, 7943−7949.

(15) Chen, H.-Y.; Hou, J.; Zhang, S.; Liang, Y.; Yang, G.; Yang, Y.; Yu, L.; Wu, Y.; Li, G. Polymer Solar Cells with Enhanced Open-Circuit Voltage and Efficiency. *Nat. Photonics* **2009**, *3*, 649−653.

(16) Chen, H.-Y.; Yang, H.; Yang, G.; Sista, S.; Zadoyan, R.; Li, G.; Yang, Y. Fast-Grown Interpenetrating Network in Poly(3-hexylth-

DOI: 10.1021/acs.jpcc.8b04192
J. Phys. Chem. C XXXX, XXX, XXX−XXX

iophene):Methanofulleres Solar Cells Processed with Additive. *J. Phys. Chem. C* **2009**, *113*, 7946−7953.
(17) Gu, Y.; Wang, C.; Russell, T. P. Multi-Length-Scale Morphologies in PCPDTBT/PCBM Bulk-Heterojunction Solar Cells. *Adv. Energy Mater.* **2012**, *2*, 683−690.
(18) Liang, Y.; Yu, L. A New Class of Semiconducting Polymers for Bulk Heterojunction Solar Cells with Exceptionally High Performance. *Acc. Chem. Res.* **2010**, *43*, 1227−1236.
(19) Park, S. H.; Roy, A.; Beaupré, S.; Cho, S.; Coates, N.; Moon, J. S.; Moses, D.; Leclerc, M.; Lee, K.; Heeger, A. J. Bulk Heterojunction Solar Cells with Internal Quantum Efficiency Approaching 100%. *Nat. Photonics* **2009**, *3*, 297−302.
(20) Manley, E. F.; Strzalka, J.; Fauvell, T. J.; Marks, T. J.; Chen, L. X. In Situ Analysis of Solvent and Additive Effects on Film Morphology Evolution in Spin-Cast Small-Molecule and Polymer Photovoltaic Materials. *Adv. Energy Mater.* **2018**, 1800611.
(21) Moon, J. S.; Takacs, C. J.; Cho, S.; Coffin, R. C.; Kim, H.; Bazan, G. C.; Heeger, A. J. *Nano Lett.* **2010**, *10*, 4005−4008.
(22) Zusan, A.; Gieseking, G.; Zerson, M.; Dyakonov, V.; Magerle, R.; Deibel, C. The Effect of Diiodooctane on the Charge Carrier Generation in Organic Solar Cells Based on the Copolymer PBDTTT-C. *Sci. Rep.* **2015**, *5*, 8286.
(23) Sun, Y.; Welch, G. C.; Leong, W. L.; Takacs, C. J.; Bazan, G. C.; Heeger, A. J. Solution-Processed Small-Molecule Solar Cells with 6.7% Efficiency. *Nat. Mater.* **2012**, *11*, 44−48.
(24) Cheng, P.; Lin, Y.; Zawacka, N. K.; Andersen, T. R.; Liu, W.; Bundgaard, E.; Jørgensen, M.; Chen, H.; Krebs, F. C.; Zhan, X. Comparison of Additive Amount Used in Spin-Coated and Roll-Coated Organic Solar Cells. *J. Mater. Chem. A* **2014**, *2*, 19542−19549.
(25) Tremolet de Villers, B. J.; O'Hara, K. A.; Ostrowski, D. P.; Biddle, P. H.; Shaheen, S. E.; Chabinyc, M. L.; Olson, D. C.; Kopidakis, N. Removal of Residual Diiodooctane Improves Photostability of High-Performance Organic Solar Cell Polymers. *Chem. Mater.* **2016**, *28*, 876−884.
(26) Xie, Y.; Hu, X.; Yin, J.; Zhang, L.; Meng, X.; Xu, G.; Ai, Q.; Zhou, W.; Chen, Y. Butanedithiol Solvent Additive Extracting Fullerenes from Donor Phase To Improve Performance and Photostability in Polymer Solar Cells. *ACS Appl. Mater. Interfaces* **2017**, *9*, 9918−9925.
(27) Jacobs, I. E.; Wang, F.; Bedolla Valdez, Z. I.; Ayala Oviedo, A. N.; Bilsky, D. J.; Moulé, A. J. Photoinduced Degradation from Trace 1,8-diiodooctane in Organic Photovoltaics. *J. Mater. Chem. C* **2018**, *6*, 219−225.
(28) Li, L.; Xiao, L.; Qin, H.; Gao, K.; Peng, J.; Cao, Y.; Liu, F.; Russell, T. P.; Peng, X. High-Efficiency Small Molecule-Based Bulk-Heterojunction Solar Cells Enhanced by Additive Annealing. *ACS Appl. Mater. Interfaces* **2015**, *7*, 21495−21502.
(29) Xiao, Z.; Yuan, Y.; Yang, B.; Vanderslice, J.; Chen, J.; Dyck, O.; Duscher, G.; Huang, J. Universal Formation of Compositionally Graded Bulk Heterojunction for Efficiency Enhancement in Organic Photovoltaics. *Adv. Mater.* **2014**, *26*, 3068−3075.
(30) Lou, S. J.; Szarko, J. M.; Xu, T.; Yu, L.; Marks, T. J.; Chen, L. X. Effects of Additives on the Morphology of Solution Phase Aggregates Formed by Active Layer Components of High-Efficiency Organic Solar Cells. *J. Am. Chem. Soc.* **2011**, *133*, 20661−20663.
(31) Liu, C.; Hu, X.; Zhong, C.; Huang, M.; Wang, K.; Zhang, Z.; Gong, X.; Cao, Y.; Heeger, A. J. The Influence of Binary Processing Additives on the Performance of Polymer Solar Cells. *Nanoscale* **2014**, *6*, 14297−14304.
(32) Zheng, Y.; Goh, T.; Fan, P.; Shi, W.; Yu, J.; Taylor, A. D. Toward Efficient Thick Active PTB7 Photovoltaic Layers Using Diphenyl Ether as a Solvent Additive. *ACS Appl. Mater. Interfaces* **2016**, *8*, 15724−15731.
(33) Yao, Y.; Hou, J.; Xu, Z.; Li, G.; Yang, Y. Effects of Solvent Mixtures on the Nanoscale Phase Separation in Polymer Solar Cells. *Adv. Funct. Mater.* **2008**, *18*, 1783−1789.
(34) Xie, L.; Lee, J. S.; Jang, Y.; Ahn, H.; Kim, Y.-h.; Kim, K. Organic Photovoltaics Utilizing a Polymer Nanofiber/Fullerene Interdigitated Bilayer Prepared by Sequential Solution Deposition. *J. Phys. Chem. C* **2016**, *120*, 12933−12940.
(35) Lee, T. H.; Park, S. Y.; Walker, B.; Ko, S.-J.; Heo, J.; Woo, H. Y.; Choi, H.; Kim, J. Y. A Universal Processing Additive for High-Performance Polymer Solar Cells. *RSC Adv.* **2017**, *7*, 7476−7482.
(36) Aguirre, J. C.; Hawks, S. A.; Ferreira, A. S.; Yee, P.; Subramaniyan, S.; Jenekhe, S. A.; Tolbert, S. H.; Schwartz, B. J. Sequential Processing for Organic Photovoltaics: Design Rules for Morphology Control by Tailored Semi-Orthogonal Solvent Blends. *Adv. Energy Mater.* **2015**, *5*, 1402020.
(37) Hawks, S. A.; Aguirre, J. C.; Schelhas, L. T.; Thompson, R. J.; Huber, R. C.; Ferreira, A. S.; Zhang, G.; Herzing, A. A.; Tolbert, S. H.; Schwartz, B. J. Comparing Matched Polymer:Fullerene Solar Cells Made by Solution-Sequential Processing and Traditional Blend Casting: Nanoscale Structure and Device Performance. *J. Phys. Chem. C* **2014**, *118*, 17413−17425.
(38) van Franeker, J. J.; Kouijzer, S.; Lou, X.; Turbiez, M.; Wienk, M. M.; Janssen, R. A. J. Depositing Fullerenes in Swollen Polymer Layers via Sequential Processing of Organic Solar Cells. *Adv. Energy Mater.* **2015**, *5*, 1500464.
(39) Scholes, D. T.; Hawks, S. A.; Yee, P. Y.; Wu, H.; Lindemuth, J. R.; Tolbert, S. H.; Schwartz, B. J. Overcoming Film Quality Issues for Conjugated Polymers Doped with F4TCNQ by Solution Sequential Processing: Hall Effect, Structural, and Optical Measurements. *J. Phys. Chem. Lett.* **2015**, *6*, 4786−4793.
(40) Scholes, D. T.; Yee, P. Y.; Lindemuth, J. R.; Kang, H.; Onorato, J.; Ghosh, R.; Luscombe, C. K.; Spano, F. C.; Tolbert, S. H.; Schwartz, B. J. The Effects of Crystallinity on Charge Transport and the Structure of Sequentially Processed F4TCNQ-Doped Conjugated Polymer Films. *Adv. Funct. Mater.* **2017**, *27*, 1702654.
(41) Manley, E. F.; Strzalka, J.; Fauvell, T. J.; Jackson, N. E.; Leonardi, M. J.; Eastham, N. D.; Marks, T. J.; Chen, L. X. In Situ GIWAXS Analysis of Solvent and Additive Effects on PTB7 Thin Film Microstructure Evolution During Spin Coating. *Adv. Mater.* **2017**, *29*, 1703933.
(42) Shin, N.; Richter, L. J.; Herzing, A. A.; Kline, R. J.; Delongchamp, D. M. Effect of Processing Additives on the Solidification of Blade-Coated Polymer/Fullerene Blend Films via In-Situ Structure Measurements. *Adv. Energy Mater.* **2013**, *3*, 938−948.
(43) Richter, L. J.; Delongchamp, D. M.; Bokel, F. A.; Engmann, S.; Chou, K. W.; Amassian, A.; Schaible, E.; Hexemer, A. In Situ Morphology Studies of the Mechanism for Solution Additive Effects on the Formation of Bulk Heterojunction Films. *Adv. Energy Mater.* **2015**, *5*, 1400975.
(44) Immergut, E. H.; Mark, H. F. Principles of Plasticization. *Adv. Chem. Ser.* **1965**, *48*, 1−26.
(45) Subramaniyan, S.; Xin, H.; Kim, F. S.; Shoaee, S.; Durrant, J. R.; Jenekhe, S. A. Effects of Side Chains on Thiazolothiazole-Based Copolymer Semiconductors for High Performance Solar Cells. *Adv. Energy Mater.* **2011**, *1*, 854−860.
(46) Yang, Y. M.; Chen, W.; Dou, L.; Chang, W.-H.; Duan, H.-S.; Bob, B.; Li, G.; Yang, Y. High-Performance Multiple-Donor Bulk Heterojunction Solar Cells. *Nat. Photonics* **2015**, *9*, 190−198.
(47) Subramaniyan, S.; Xin, H.; Kim, F. S.; Jenekhe, S. A. New Thiazolothiazole Copolymer Semiconductors for Highly Efficient Solar Cells. *Macromolecules* **2011**, *44*, 6245−6248.
(48) Papanu, J. S.; Hess, D. W.; Bell, A. T.; Soane, D. S. In Situ Ellipsometry to Monitor Swelling and Dissolution of Thin Polymer Films. *J. Electrochem. Soc.* **1989**, *136*, 1195−1200.
(49) Ng, A.; Li, C. H.; Fung, M. K.; Djurišić, A. B.; Zapien, J. A.; Chan, W. K.; Cheung, K. Y.; Wong, W.-Y. Accurate Determination of the Index of Refraction of Polymer Blend Films by Spectroscopic Ellipsometry. *J. Phys. Chem. C* **2010**, *114*, 15094−15101.
(50) Zhang, G.; Hawks, S. A.; Ngo, C.; Schelhas, L. T.; Scholes, D. T.; Kang, H.; Aguirre, J. C.; Tolbert, S. H.; Schwartz, B. J. Extensive Penetration of Evaporated Electrode Metals into Fullerene Films: Intercalated Metal Nanostructures and Influence on Device Architecture. *ACS Appl. Mater. Interfaces* **2015**, *7*, 25247−25258.

DOI: 10.1021/acs.jpcc.8b04192
J. Phys. Chem. C XXXX, XXX, XXX−XXX

(51) Kong, J.; Hwang, I.-W.; Lee, K. Top-Down Approach for Nanophase Reconstruction in Bulk Heterojunction Solar Cells. *Adv. Mater.* **2014**, *26*, 6275−6283.
(52) Ayzner, A. L.; Tassone, C. J.; Tolbert, S. H.; Schwartz, B. J. Reappraising the Need for Bulk Heterojunctions in Polymer-Fullerene Photovoltaics: The Role of Carrier Transport in All-Solution-Processed P3HT/PCBM Bilayer Solar Cells. *J. Phys. Chem. C* **2009**, *113*, 20050−20060.
(53) Molebase, 1,8-Diiodooctane. http://www.molbase.com/en/properties{_}24772-63-2-moldata-48193.html (accessed Mar. 24, 2017).
(54) Ye, L.; Jing, Y.; Guo, X.; Sun, H.; Zhang, S.; Zhang, M.; Huo, L.; Hou, J. Remove the Residual Additives toward Enhanced Efficiency with Higher Reproducibility in Polymer Solar Cells. *J. Phys. Chem. C* **2013**, *117*, 14920−14928.
(55) Molebase, 1,8-Octanedithiol. http://www.molbase.com/en/1191-62-4-moldata-55275.html (accessed Mar. 24, 2017).
(56) PubChem, 1,2-Dichlorobenzene. https://pubchem.ncbi.nlm.nih.gov/compound/7239 (accessed Mar. 24, 2017).
(57) Bruggeman, V. D. A. G. Berechnung Verschiedener Physikalischer Konstanten von Heterogenen Substanzen. I. Dielektrizitätskonstanten und Leitfähigkeiten der Mischkörper aus Isotropen Substanzen. *Ann. Phys.* **1935**, *416*, 665−679.
(58) Rogers, C. E.; Stannett, V.; Szwarc, M. The Sorption of Organic Vapors by Polyethylene. *J. Phys. Chem.* **1959**, *63*, 1406−1413.
(59) Brown, H. R. Flory-Huggins-Rehner Theory and the Swelling of Semicrystalline Polymers by Organic Fluids. *J. Polym. Sci., Polym. Phys. Ed.* **1978**, *16*, 1887−1889.
(60) Zhang, G.; Huber, R. C.; Ferreira, A. S.; Boyd, S. D.; Luscombe, C. K.; Tolbert, S. H.; Schwartz, B. J. Crystallinity Effects in Sequentially Processed and Blend-Cast Bulk-Heterojunction Polymer/Fullerene Photovoltaics. *J. Phys. Chem. C* **2014**, *118*, 18424−18435.
(61) Ratcliff, E. L.; Jenkins, J. L.; Nebesny, K.; Armstrong, N. R. Films for Photovoltaic Applications. *Chem. Mater.* **2008**, *20*, 5796−5806.
(62) Xu, Z.; Chen, L.-M.; Yang, G.; Huang, C.-H.; Hou, J.; Wu, Y.; Li, G.; Hsu, C.-S.; Yang, Y. Vertical Phase Separation in Poly(3-hexylthiophene): Fullerene Derivative Blends and its Advantage for Inverted Structure Solar Cells. *Adv. Funct. Mater.* **2009**, *19*, 1227−1234.
(63) Orimo, A.; Masuda, K.; Honda, S.; Benten, H.; Ito, S.; Ohkita, H.; Tsuji, H. Surface Segregation at the Aluminum Interface of Poly(3-hexylthiophene)/Fullerene Solar Cells. *Appl. Phys. Lett.* **2010**, *96*, 043305.
(64) Lee, K. H.; Schwenn, P. E.; Smith, A. R. G.; Cavaye, H.; Shaw, P. E.; James, M.; Krueger, K. B.; Gentle, I. R.; Meredith, P.; Burn, P. L. Morphology of All-Solution-Processed "Bilayer" Organic Solar Cells. *Adv. Mater.* **2011**, *23*, 766−770.
(65) Lee, K. H.; Zhang, Y.; Burn, P. L.; Gentle, I. R.; James, M.; Nelson, A.; Meredith, P. Correlation of Diffusion and Performance in Sequentially Processed P3HT/PCBM Heterojunction Films by Time-Resolved Neutron Reflectometry. *J. Mater. Chem. C* **2013**, *1*, 2593−2598.
(66) Tao, C.; Aljada, M.; Shaw, P. E.; Lee, K. H.; Cavaye, H.; Balfour, M. N.; Borthwick, R. J.; James, M.; Burn, P. L.; Gentle, I. R.; Meredith, P. Controlling Hierarchy in Solution-Processed Polymer Solar Cells Based on Crosslinked P3HT. *Adv. Energy Mater.* **2013**, *3*, 105−112.
(67) Das, S.; Keum, J. K.; Browning, J. F.; Gu, G.; Yang, B.; Dyck, O.; Do, C.; Chen, W.; Chen, J.; Ivanov, I. N.; et al. Correlating High Power Conversion Efficiency of PTB7:PC71BM Inverted Organic Solar Cells with Nanoscale Structures. *Nanoscale* **2015**, *7*, 15576−15583.
(68) Flory, P. J. Thermodynamics of High Polymer Solutions. *J. Chem. Phys.* **1942**, *10*, 51−61.
(69) PubChem, Dichloromethane. https://pubchem.ncbi.nlm.nih.gov/compound/6344 (accessed Mar. 24, 2017).
(70) Gevaerts, V. S.; Koster, L. J. A.; Wienk, M. M.; Janssen, R. A. J. Discriminating Between Bilayer and Bulk Heterojunction Polymer: Fullerene Solar Cells Using the External Quantum Efficiency. *ACS Appl. Mater. Interfaces* **2011**, *3*, 3252−3255.
(71) Moon, J. S.; Takacs, C. J.; Sun, Y.; Heeger, A. J. Spontaneous Formation of Bulk Heterojunction Nanostructures: Multiple Routes to Equivalent Morphologies. *Nano Lett.* **2011**, *11*, 1036−1039.
(72) Nardes, A. M.; Ayzner, A. L.; Hammond, S. R.; Ferguson, A. J.; Schwartz, B. J.; Kopidakis, N. Photoinduced Charge Carrier Generation and Decay in Sequentially Deposited Polymer/Fullerene Layers: Bulk Heterojunction vs Planar Interface. *J. Phys. Chem. C* **2012**, *116*, 7293−7305.
(73) Venkatesan, S.; Adhikari, N.; Chen, J.; Ngo, E. C.; Dubey, A.; Galipeau, D. W.; Qiao, Q. Interplay of Domain Purity on Charge Transport and Recombination Dynamics in Polymer Solar Cells. *Nanoscale* **2014**, *6*, 1011−1019.
(74) Wan, Q.; Guo, X.; Wang, Z.; Li, W.; Guo, B.; Ma, W.; Zhang, M.; Li, Y. 10.8% Efficiency Polymer Solar Cells Based on PTB7-Th and PC71BM via Binary Solvent Additives Treatment. *Adv. Funct. Mater.* **2016**, *26*, 6635−6640.
(75) Zheng, Y.; Wang, G.; Huang, D.; Kong, J.; Goh, T.; Huang, W.; Yu, J.; Taylor, A. D. Binary Solvent Additives Treatment Boosts the Efficiency of PTB7:PCBM Polymer Solar Cells to Over 9.5%. *Solar RRL* **2018**, *2*, 1700144.
(76) Kim, W.; Kim, J. K.; Kim, E.; Ahn, T. K.; Wang, D. H.; Park, J. H. Conflicted Effects of a Solvent Additive on PTB7:PC71BM Bulk Heterojunction Solar Cells. *J. Phys. Chem. C* **2015**, *119*, 5954−5961.
(77) Wang, W.; Song, L.; Magerl, D.; Moseguí González, D.; Körstgens, V.; Philipp, M.; Moulin, J. F.; Müller-Buschbaum, P. Influence of Solvent Additive 1,8-Octanedithiol on P3HT:PCBM Solar Cells. *Adv. Funct. Mater.* **2018**, *28*, 1800209.
(78) Krauskopf, L. G.; Godwin, A. *PVC Handb.*; 2005; pp 173−193.
(79) Godwin, A. D.; Krauskopf, L. G. In *Handbook of Vinyl Formulating*, 2nd ed.; Grossman, R. F., Ed.; John Wiley & Sons, Inc., 2008; Chapter Seven, pp 173−238.
(80) PubChem, 1-Chloronaphthalene. https://pubchem.ncbi.nlm.nih.gov/compound/1-chloronaphthalene{\#}section/Top (accessed Mar. 24.017).
(81) Ambrose, D.; Ellender, J. H.; Sprake, C. H. S.; Townsend, R. Thermodynamic Properties of Oxygen Compounds of Organic Vapour Pressures of Some Ethers. *J. Chem. Thermodyn.* **1976**, *8*, 165−178.
(82) Zhao, J.; Zhao, S.; Xu, Z.; Qiao, B.; Huang, D.; Zhao, L.; Li, Y.; Zhu, Y.; Wang, P. Revealing the Effect of Additives with Different Solubility on the Morphology and the Donor Crystalline Structures of Organic Solar Cells. *ACS Appl. Mater. Interfaces* **2016**, *8*, 18231−18237.
(83) Wang, D. H.; Kyaw, A. K. K.; Pouliot, J. R.; Leclerc, M.; Heeger, A. J. Enhanced Power Conversion Efficiency of Low Band-Gap Polymer Solar Cells by Insertion of Optimized Binary Processing Additives. *Adv. Energy Mater.* **2014**, *4*, 1300835.
(84) Cehreli, S.; Tatli, B.; Bagman, P. (Liquid + Liquid) Equilibria of (Water + Propionic Acid + Cyclohexanone) at Several Temperatures. *J. Chem. Thermodyn.* **2005**, *37*, 1288−1293.
(85) Liu, F.; Zhao, W.; Tumbleston, J. R.; Wang, C.; Gu, Y.; Wang, D.; Briseno, A. L.; Ade, H.; Russell, T. P. Understanding the Morphology of PTB7:PCBM Blends in Organic Photovoltaics. *Adv. Energy Mater.* **2014**, *4*, 1301377.

DOI: 10.1021/acs.jpcc.8b04192
J. Phys. Chem. C XXXX, XXX, XXX−XXX